SUPPLEMENTARY DATA

**Supplementary Figure 1.** Largest genetic principal component against second-largest genetic principal component generated using all individuals included in the primary analysis, coloured by country of enrolment.

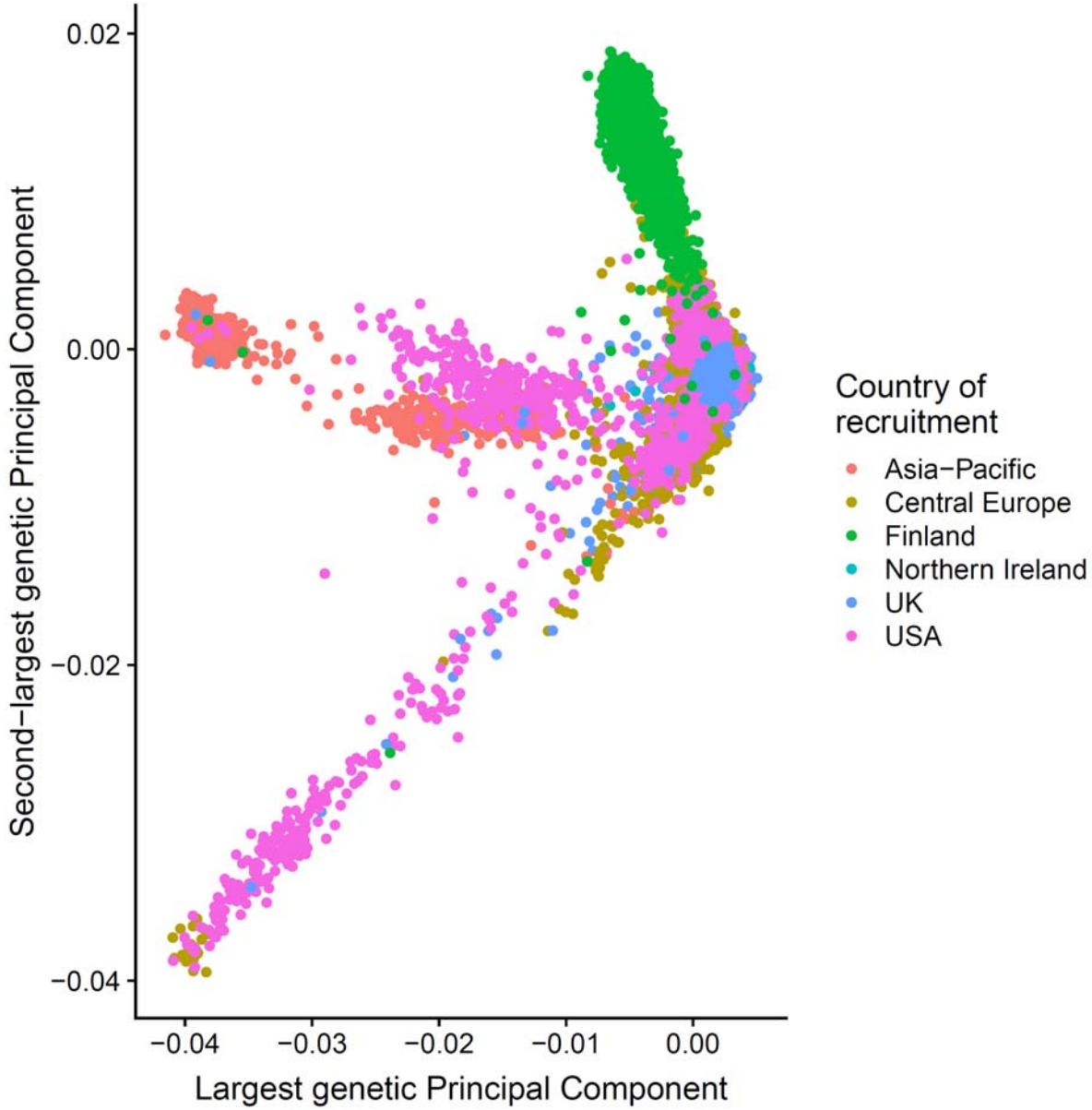

SUPPLEMENTARY DATA

**Supplementary Figure 2.** Concordance of HiBag imputed versus directly genotyped classical HLA alleles. Concordance is defined as identical 4 digit HLA classical allele at both chromosomes.

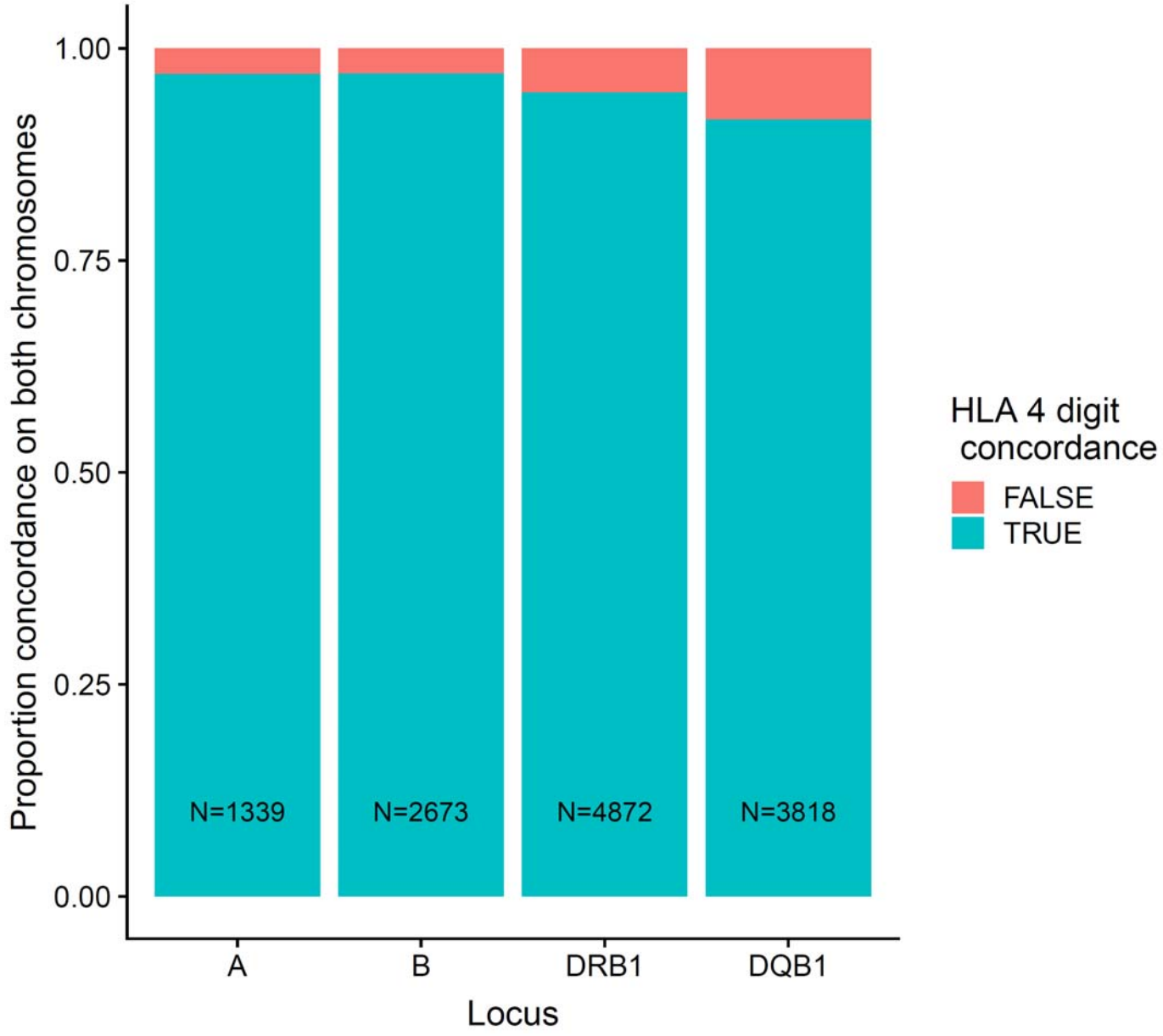

SUPPLEMENTARY DATA

**Supplementary Figure 3.** All 55 non-HLA type 1 diabetes associated variants, showing on the left hand panel the log-odds ratios for the minor allele for those diagnosed at <7 years old (red circle; log-odds ratio age-at-diagnosis +/- 95%CI), 7-13 years old (green circle; log-odds ratio age-at-diagnosis 7-13+/- 95%CI) and ≥13 years old (blue circle log-odds ratio age-at-diagnosis ≥13+/- 95%CI), from a multinomial logistic regression; the dashed red line shows a log-odds ratio of 0. The right panel shows the association statistics from a likelihood ratio test comparing a multinomial logistic regression constraining the log-odds ratios from the <7 and ≥13 groups to be equal compared to an unconstrained model. Red dotted line shows threshold for nominally significant heterogeneity between groups ($p<0.05$), red solid line shows threshold for false discovery rate of <0.1, red dashed line shows threshold for Bonferroni-corrected significant heterogeneity.

SUPPLEMENTARY DATA

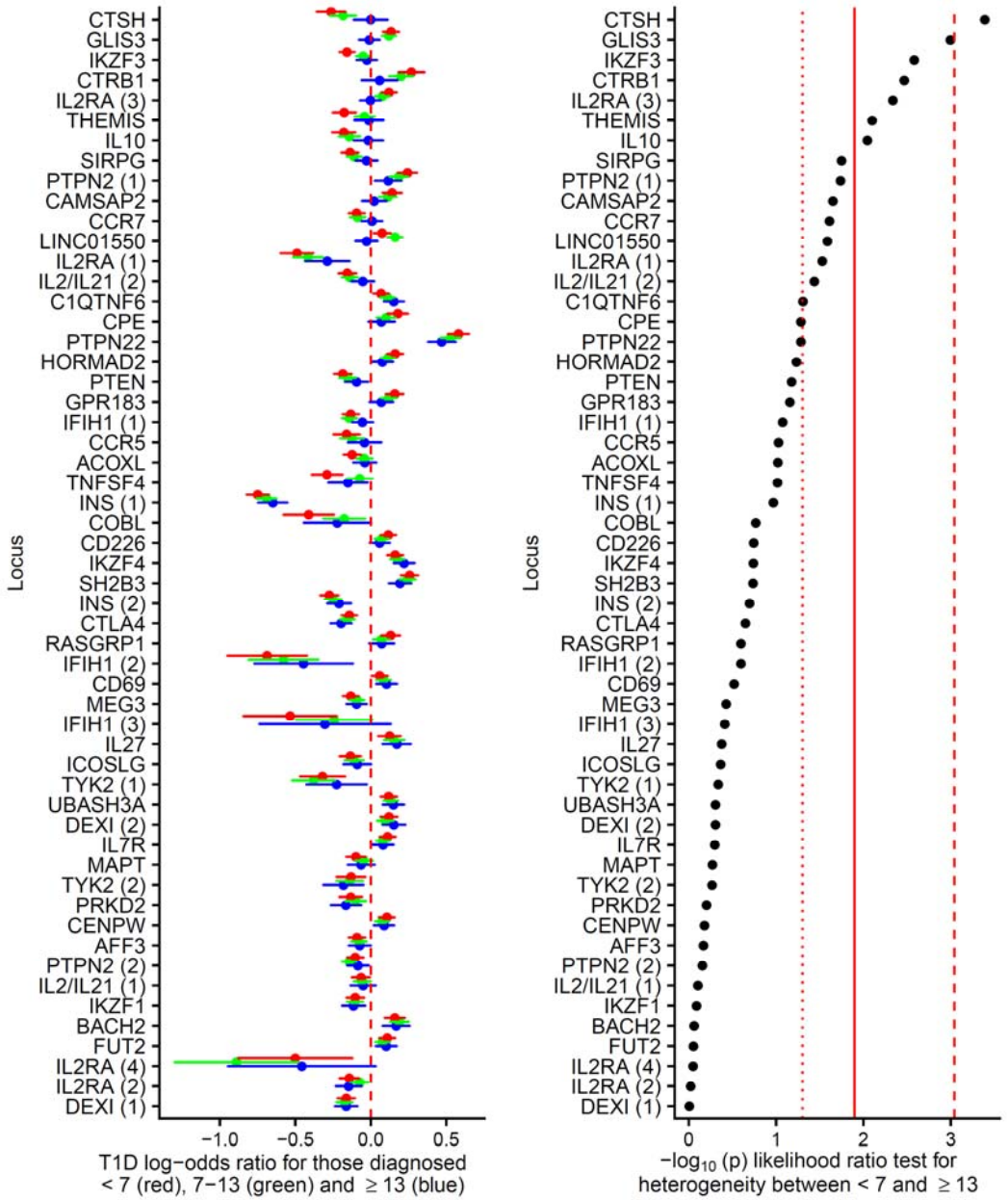

SUPPLEMENTARY DATA

**Supplementary Figure 4.** All 55 non-HLA type 1 diabetes associated variants examined using only individuals from the UK or Northern Ireland, showing on the left hand panel the log-odds ratios for the minor allele for those diagnosed at <7 years old (red circle; log-odds ratio age-at-diagnosis +/- 95%CI), 7-13 years old (green circle; log-odds ratio age-at-diagnosis 7-13+/- 95%CI) and ≥13 years old (blue circle log-odds ratio age-at-diagnosis >13+/- 95%CI), from a multinomial logistic regression; the dashed red line shows a log-odds ratio of 0. The right panel shows the association statistics from a likelihood ratio test comparing a multinomial logistic regression constraining the log-odds ratios from the <7 and ≥13 groups to be equal compared to an unconstrained model. Red dotted line shows threshold for nominally significant heterogeneity between groups ($p<0.05$), red solid line shows threshold for false discovery rate of <0.1, red dashed line shows threshold for Bonferroni-corrected significant heterogeneity.

SUPPLEMENTARY DATA

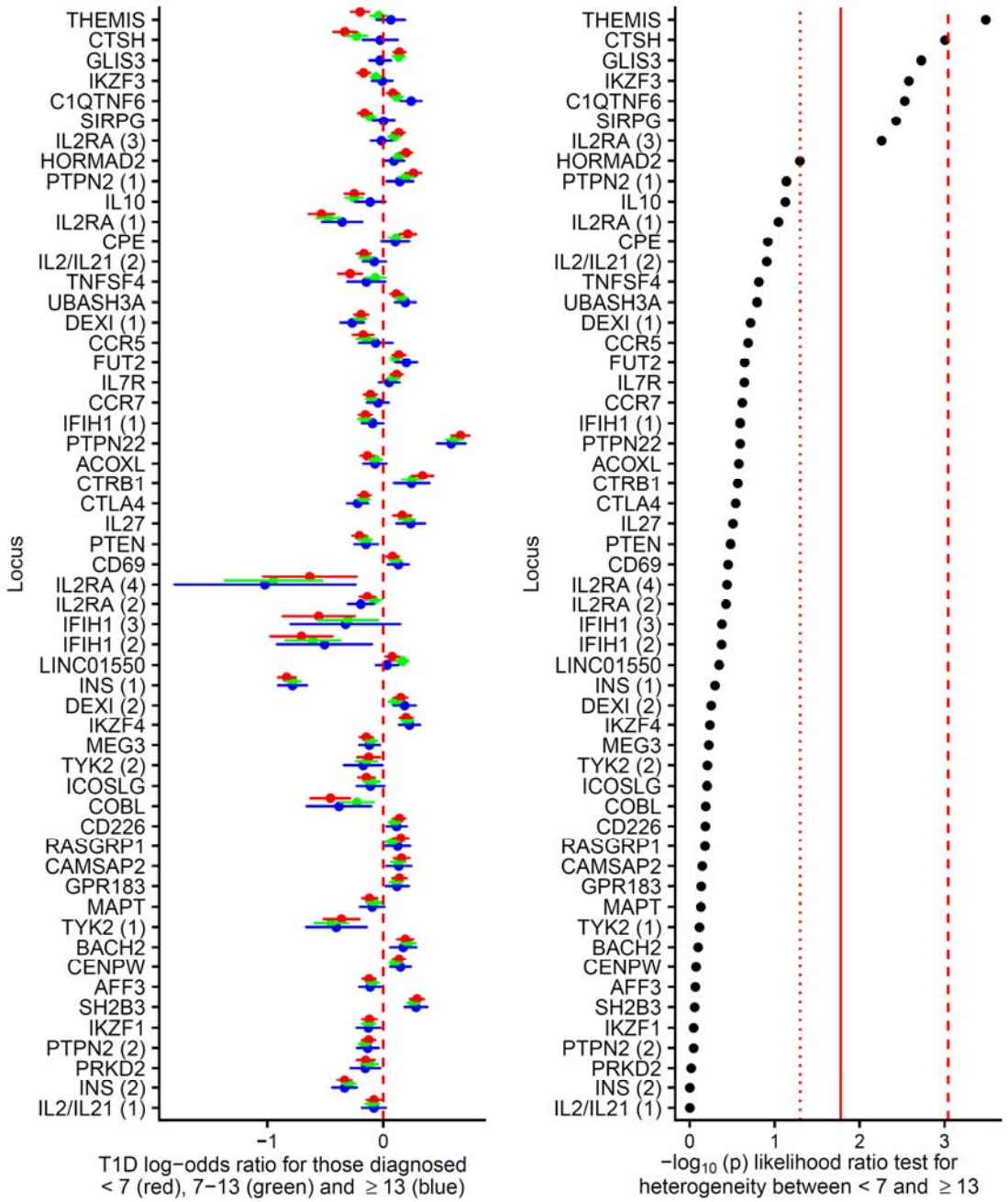

SUPPLEMENTARY DATA

**Supplementary Figure 5.** All 55 non-HLA type 1 diabetes associated variants, showing on the left hand panel the log-odds ratios for the minor allele for those diagnosed at <6 years old (red circle; log-odds ratio age-at-diagnosis +/- 95%CI), 6-13 years old (green circle; log-odds ratio age-at-diagnosis 6-13+/- 95%CI) and ≥13 years old (blue circle log-odds ratio age-at-diagnosis ≥13+/- 95%CI) from a multinomial logistic regression; the dashed red line shows a log-odds ratio of 0. The right panel shows the association statistics from a likelihood ratio test comparing a multinomial logistic regression constraining the log-odds ratios from the <6 and ≥13 groups to be equal compared to an unconstrained model. Red dotted line shows threshold for nominally significant heterogeneity between groups ($p<0.05$), red solid line shows threshold for false discovery rate of <0.1, red dashed line shows threshold for Bonferroni-corrected significant heterogeneity.

SUPPLEMENTARY DATA

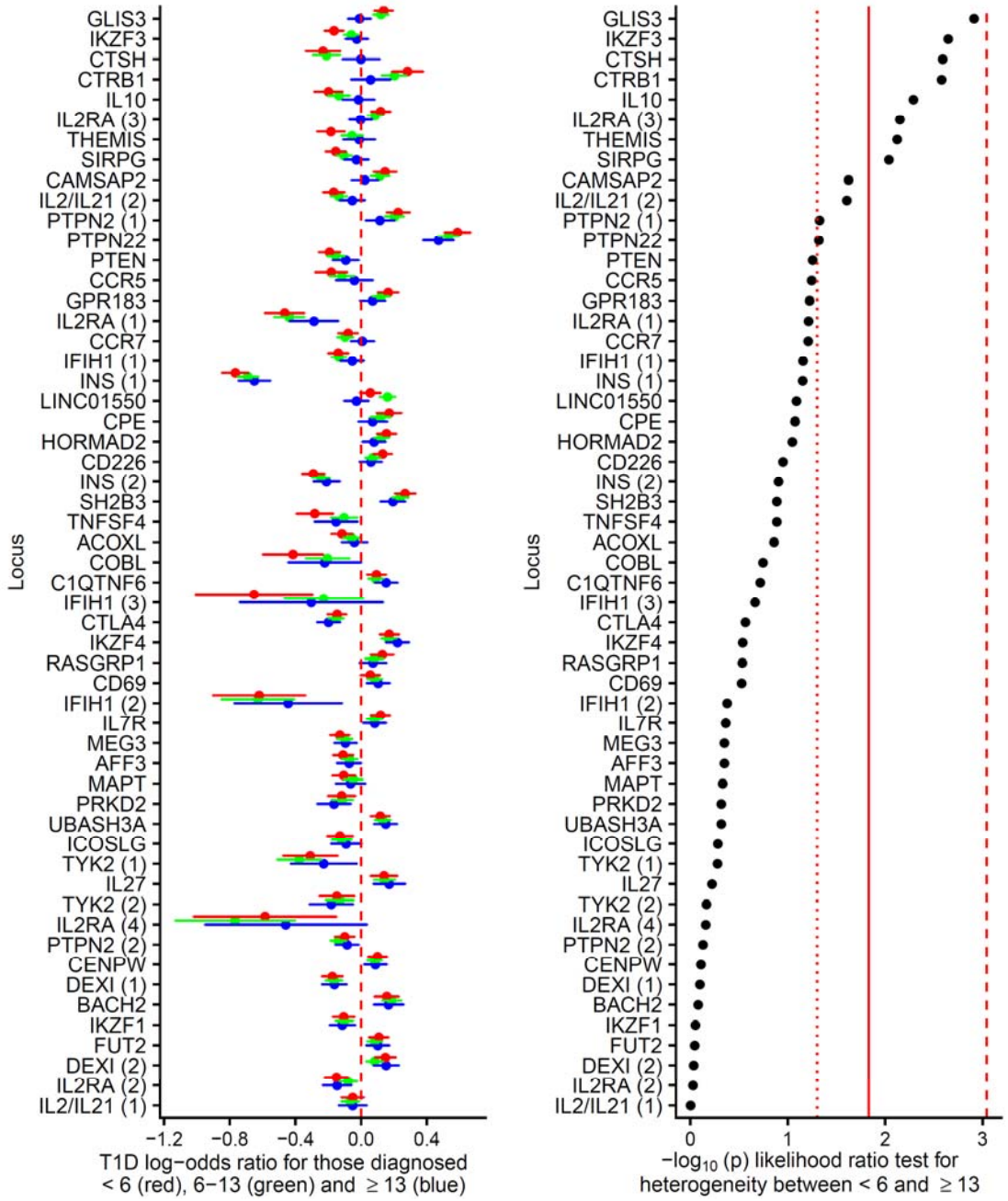

SUPPLEMENTARY DATA

**Supplementary Figure 6.** All 55 non-HLA type 1 diabetes associated variants, showing on the left hand panel the log-odds ratios for the minor allele for those diagnosed at <5 years old (red circle; log-odds ratio age-at-diagnosis +/- 95%CI), 5-13 years old (green circle; log-odds ratio age-at-diagnosis 5-13+/- 95%CI) and ≥13 years old (blue circle log-odds ratio age-at-diagnosis ≥13+/- 95%CI) from a multinomial logistic regression; the dashed red line shows a log-odds ratio of 0. The right panel shows the association statistics from a likelihood ratio test comparing a multinomial logistic regression constraining the log-odds ratios from the <5 and ≥13 groups to be equal compared to an unconstrained model. Red dotted line shows threshold for nominally significant heterogeneity between groups ($p<0.05$), red solid line shows threshold for false discovery rate of <0.1, red dashed line shows threshold for Bonferroni-corrected significant heterogeneity.

SUPPLEMENTARY DATA

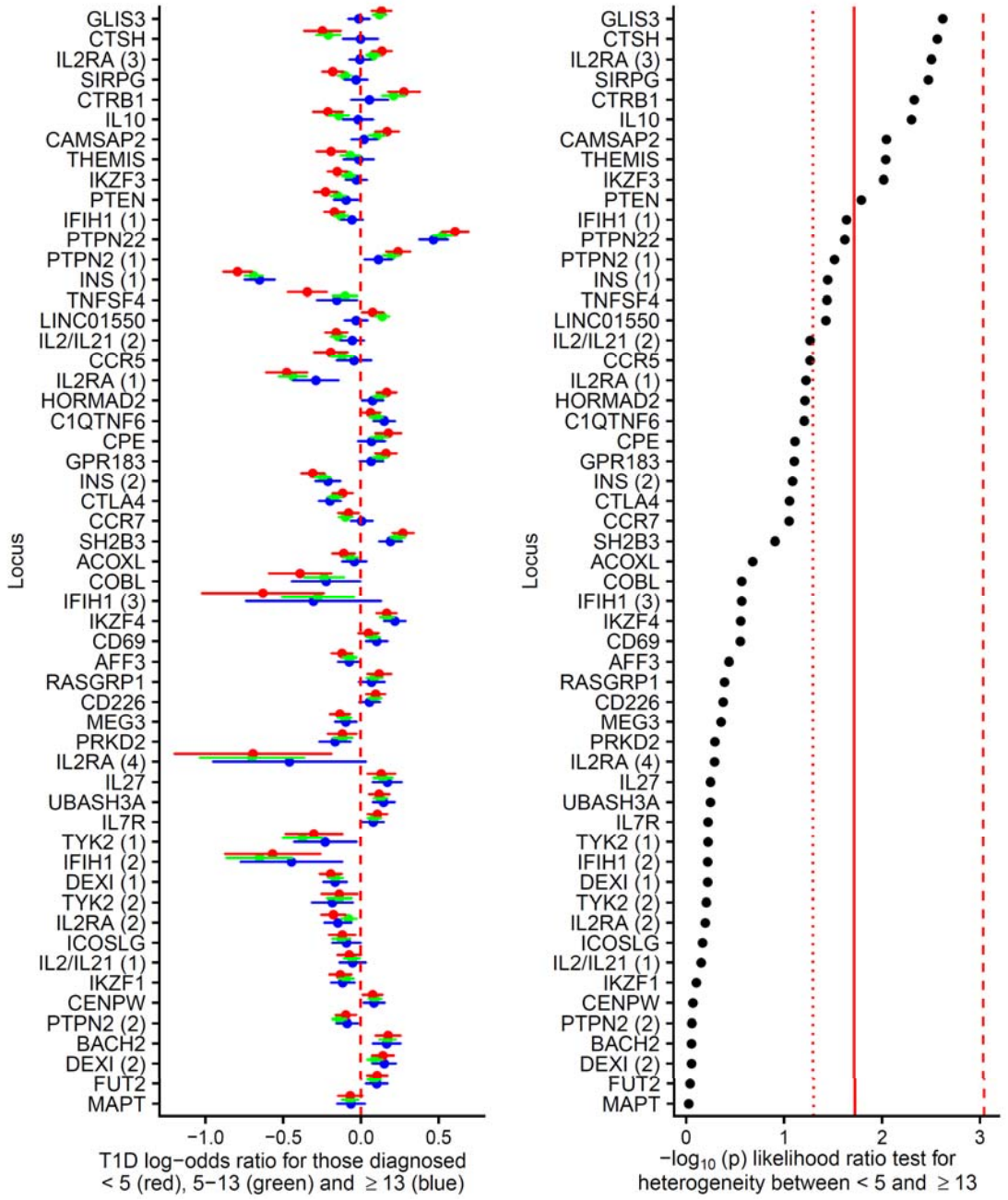

SUPPLEMENTARY DATA

**Supplementary Figure 7.** Minor allele frequency of the index variant near the *CTSH* gene for controls and individuals diagnosed at various ages.

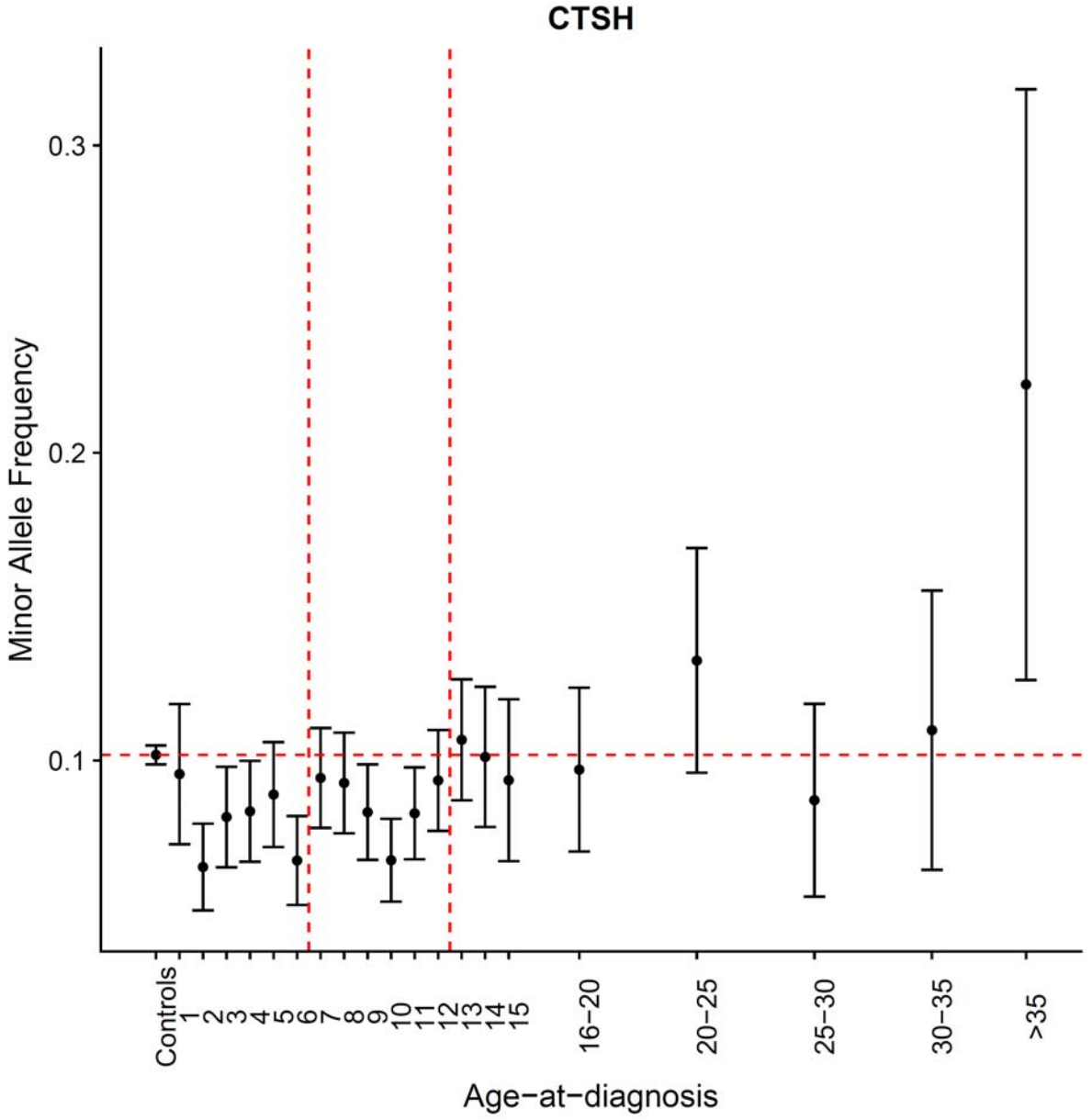

SUPPLEMENTARY DATA

**Supplementary Figure 8.** Minor allele frequency of the index variant near the *GLIS3* gene for controls and individuals diagnosed at various ages.

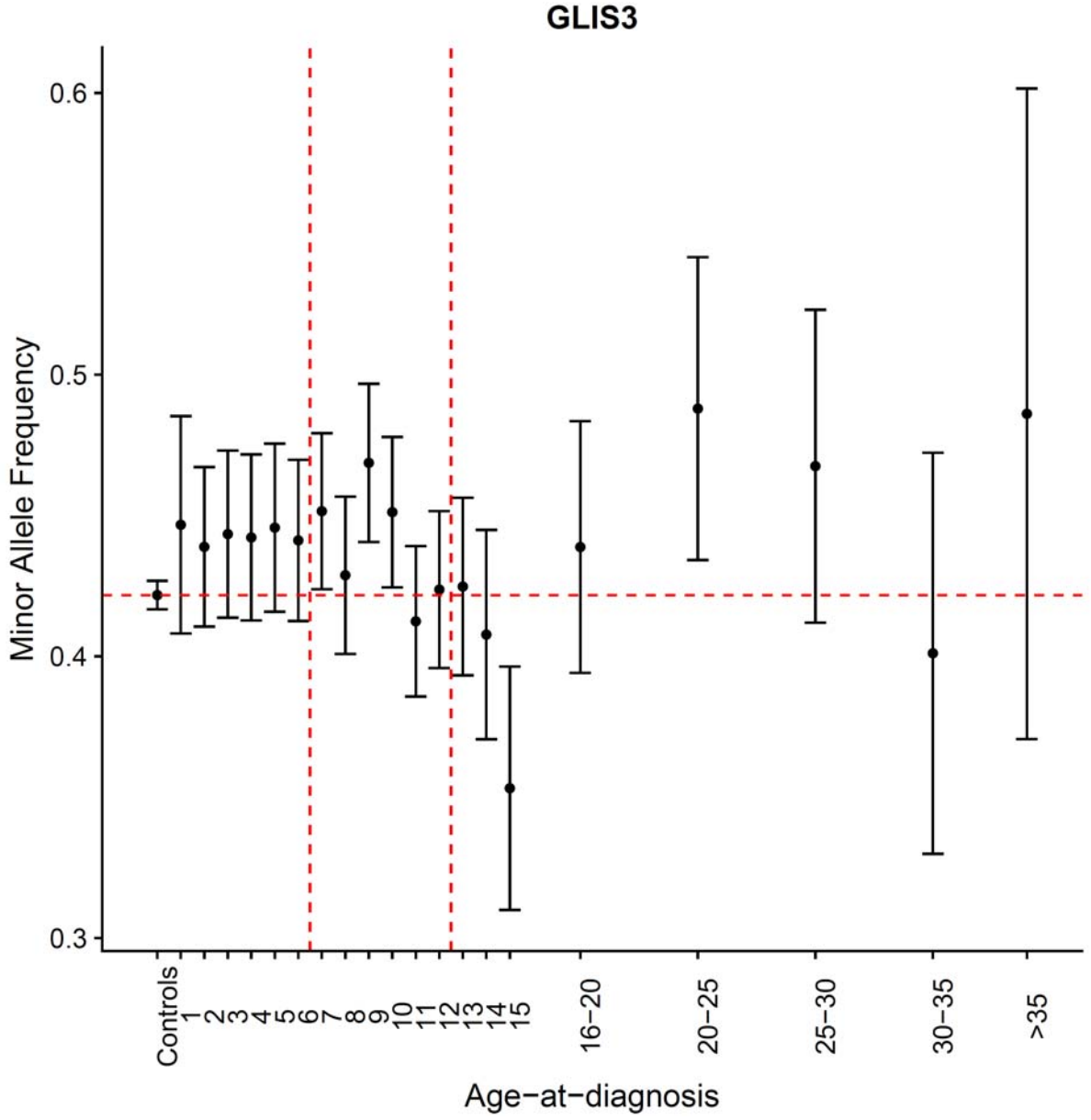

SUPPLEMENTARY DATA

**Supplementary Figure 9.** Minor allele frequency of the index variant near the *IKZF3* gene for controls and individuals diagnosed at various ages.

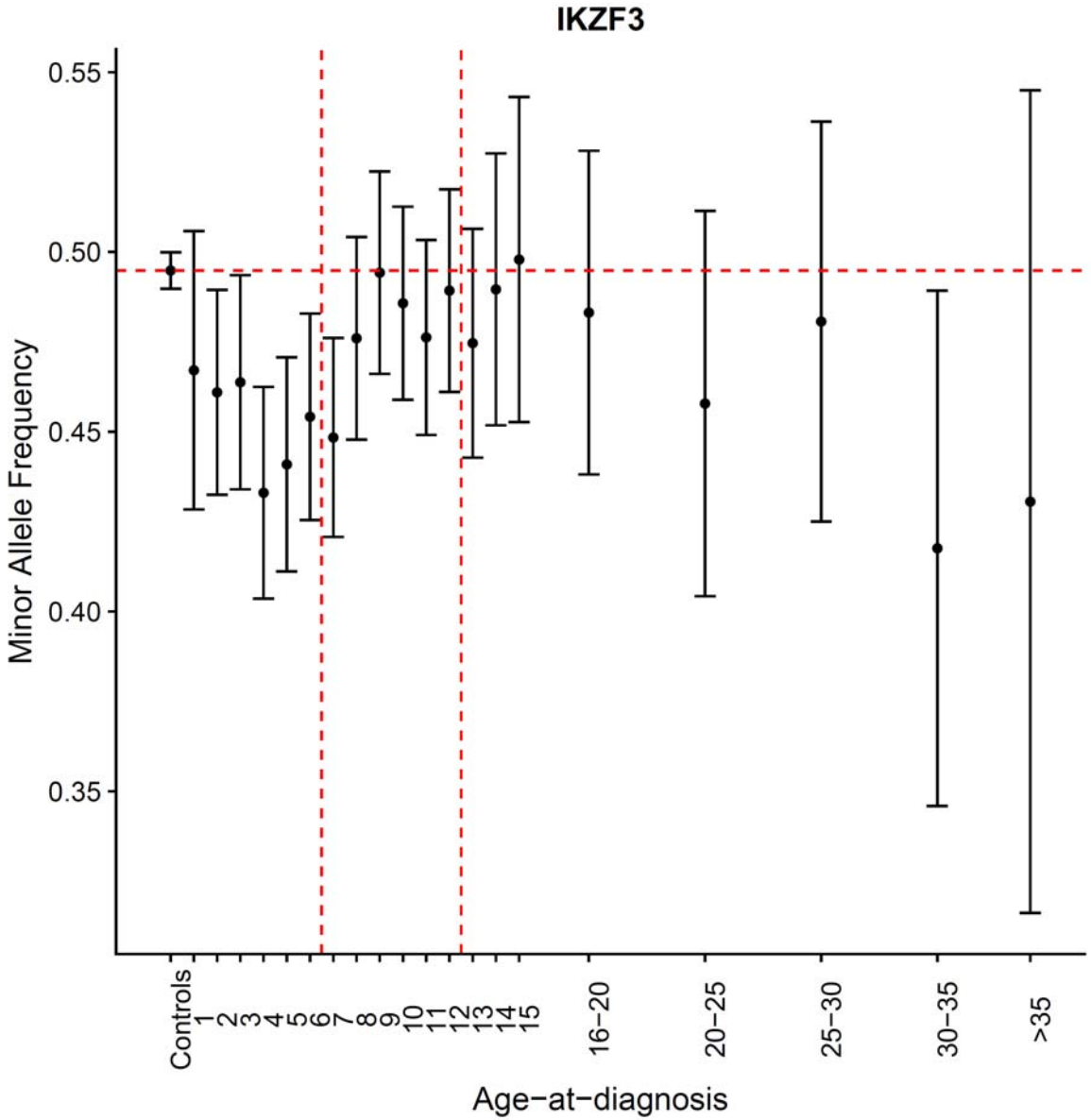

SUPPLEMENTARY DATA

**Supplementary Figure 10.** Minor allele frequency of the index variant near the *IL2RA* gene (third index variant) for controls and individuals diagnosed at various ages.

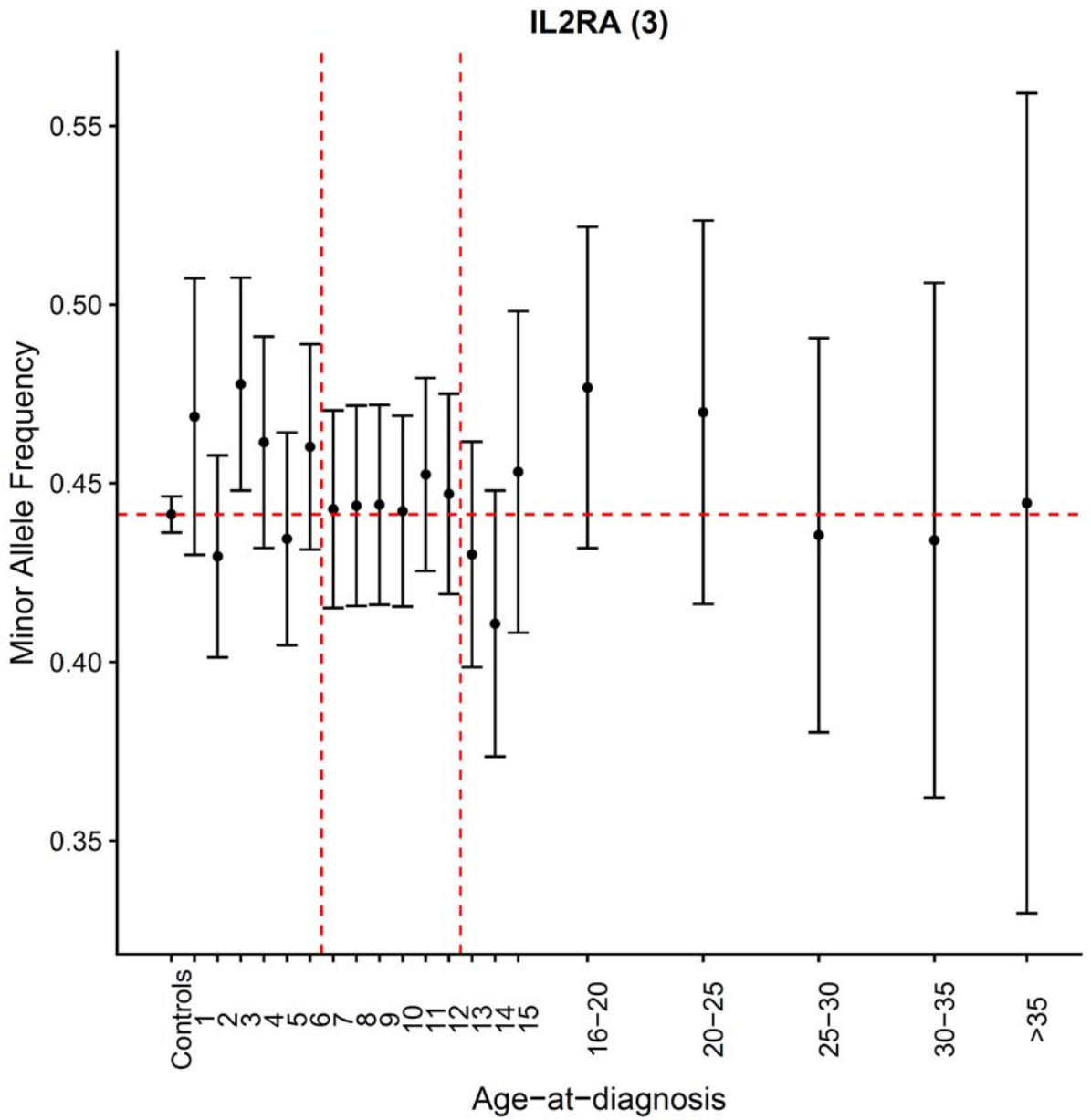

SUPPLEMENTARY DATA

**Supplementary Figure 11.** Minor allele frequency of the index variant near the *THEMIS* gene for controls and individuals diagnosed at various ages.

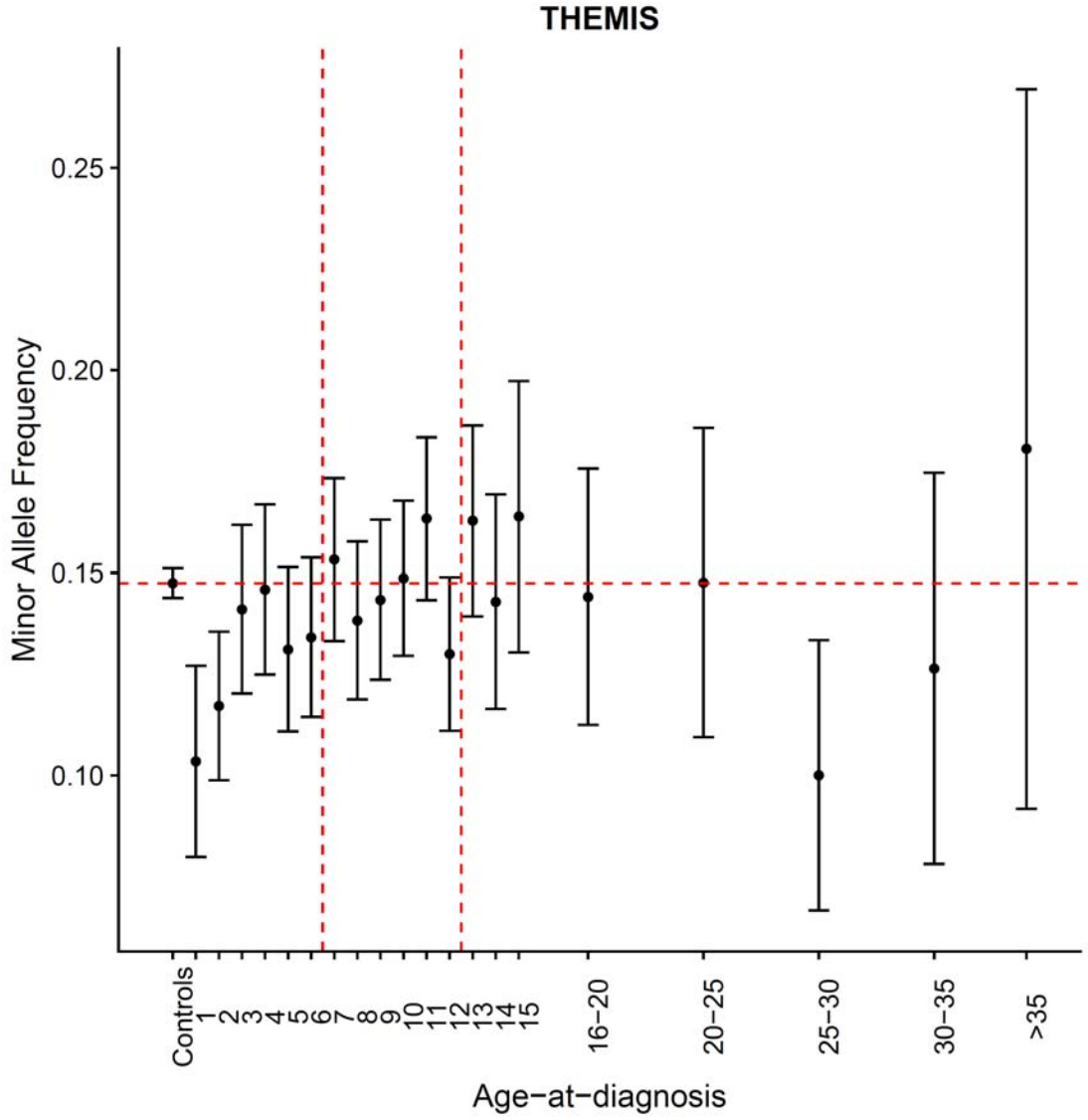

SUPPLEMENTARY DATA

**Supplementary Figure 12.** Minor allele frequency of the index variant near the *IL10* gene for controls and individuals diagnosed at various ages.

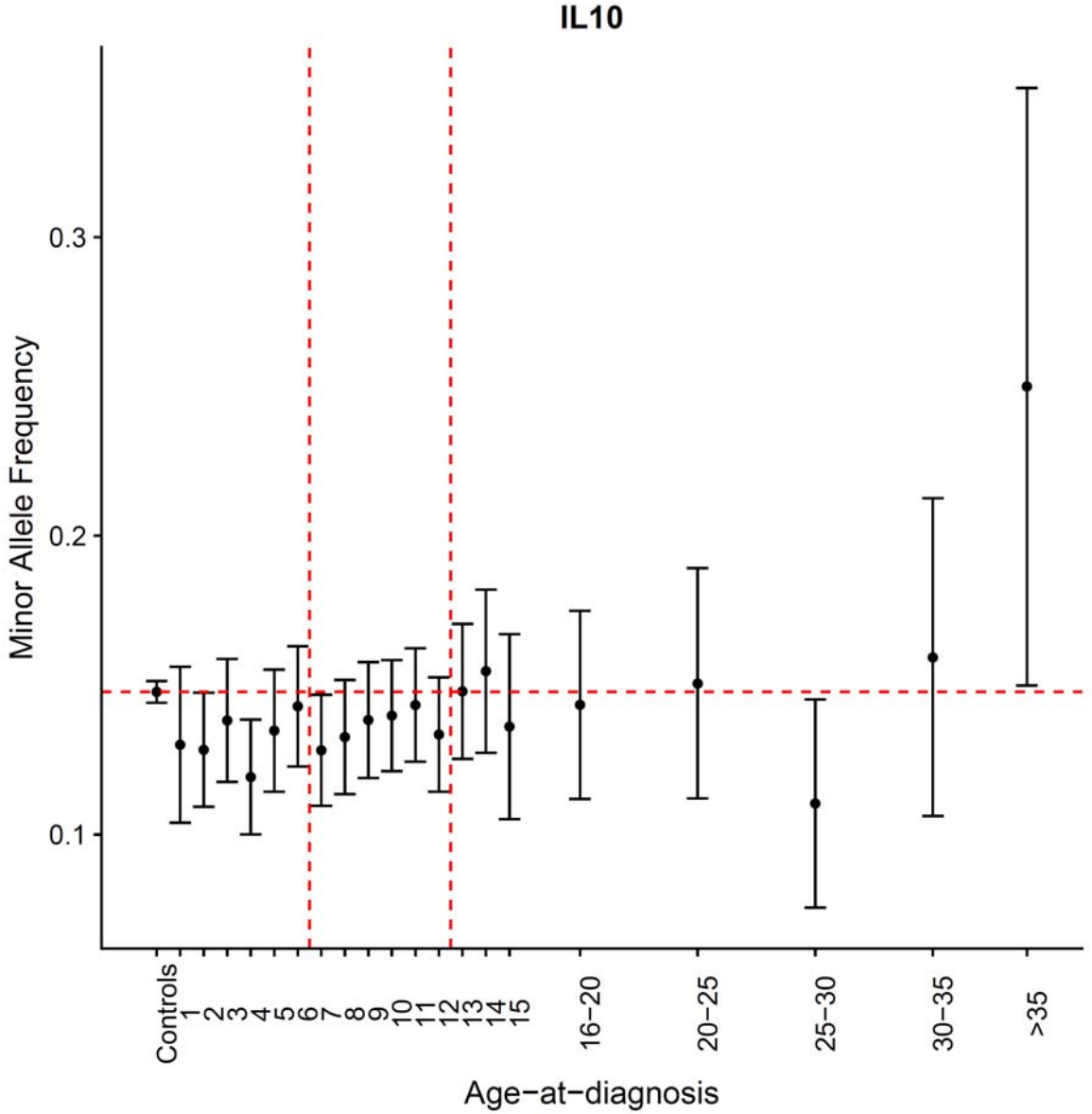

SUPPLEMENTARY DATA

**Supplementary Figure 13.** Top panel: association absolute z scores from whole blood eQTL study examining variant effects on GLIS3 mRNA levels, coloured by LD $r^2$ to the most strongly associated variant with GLIS3 mRNA expression. Bottom panel: association absolute z scores from logistic regression examining variant associations with type 1 diabetes risk diagnosed at <7 years, using individuals from the UK and Northern Ireland only and adjusting for the five largest principal components as derived from genotype data, coloured by LD $r^2$ to the most strongly associated variant with GLIS3 mRNA. Shows most associated disease risk variants are not in high LD with the most associated GLIS3 whole blood eQTLs.

SUPPLEMENTARY DATA

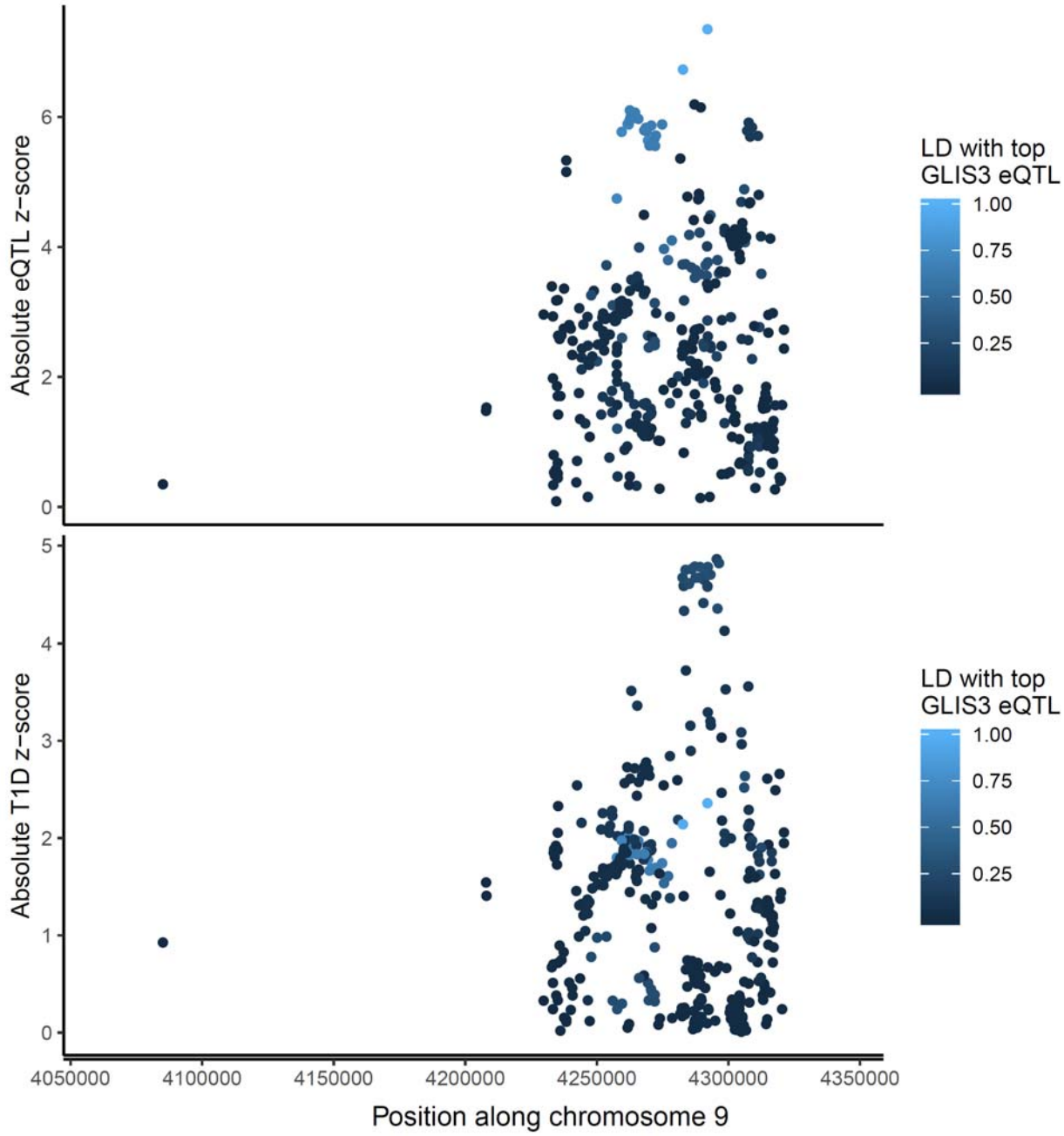

SUPPLEMENTARY DATA

**Supplementary Figure 14.** Top panel: association absolute z-scores from whole blood eQTL study examining variant effects on IL10 mRNA levels, coloured by LD $r^2$ to the most strongly associated variant with IL10 mRNA expression. Bottom panel: association absolute z scores from logistic regression examining variant associations with type 1 diabetes risk diagnosed at <7 years, using individuals from the UK and Northern Ireland only and adjusting for the five largest principal components as derived from genotype data, coloured by LD $r^2$ to the most strongly associated variant with IL10 mRNA. Shows most associated disease risk variants are not in high LD with the most associated IL10 whole blood eQTLs.

SUPPLEMENTARY DATA

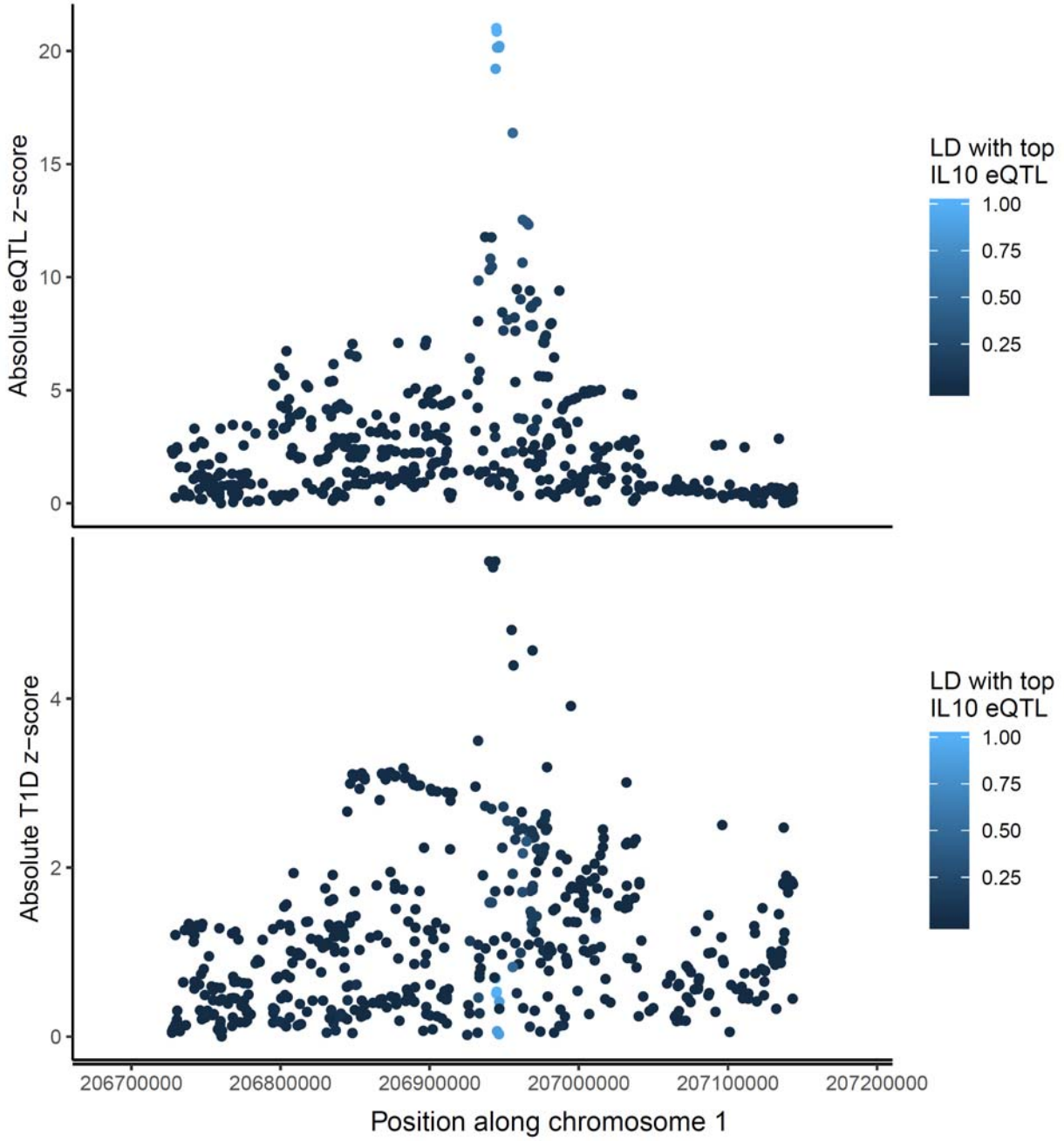

SUPPLEMENTARY DATA

**Supplementary Figure 15.** Top panel: association absolute z-scores from whole blood eQTL study examining variant effects on IL24 mRNA levels, coloured by LD $r^2$ to the most strongly associated variant with IL24 mRNA expression. Bottom panel: association absolute z scores from logistic regression examining variant associations with type 1 diabetes risk diagnosed at <7 years, using individuals from the UK and Northern Ireland only and adjusting for the five largest principal components as derived from genotype data, coloured by LD $r^2$ to the most strongly associated variant with IL24 mRNA. Shows most associated disease risk variants are not in high LD with the most associated IL24 whole blood eQTLs.

SUPPLEMENTARY DATA

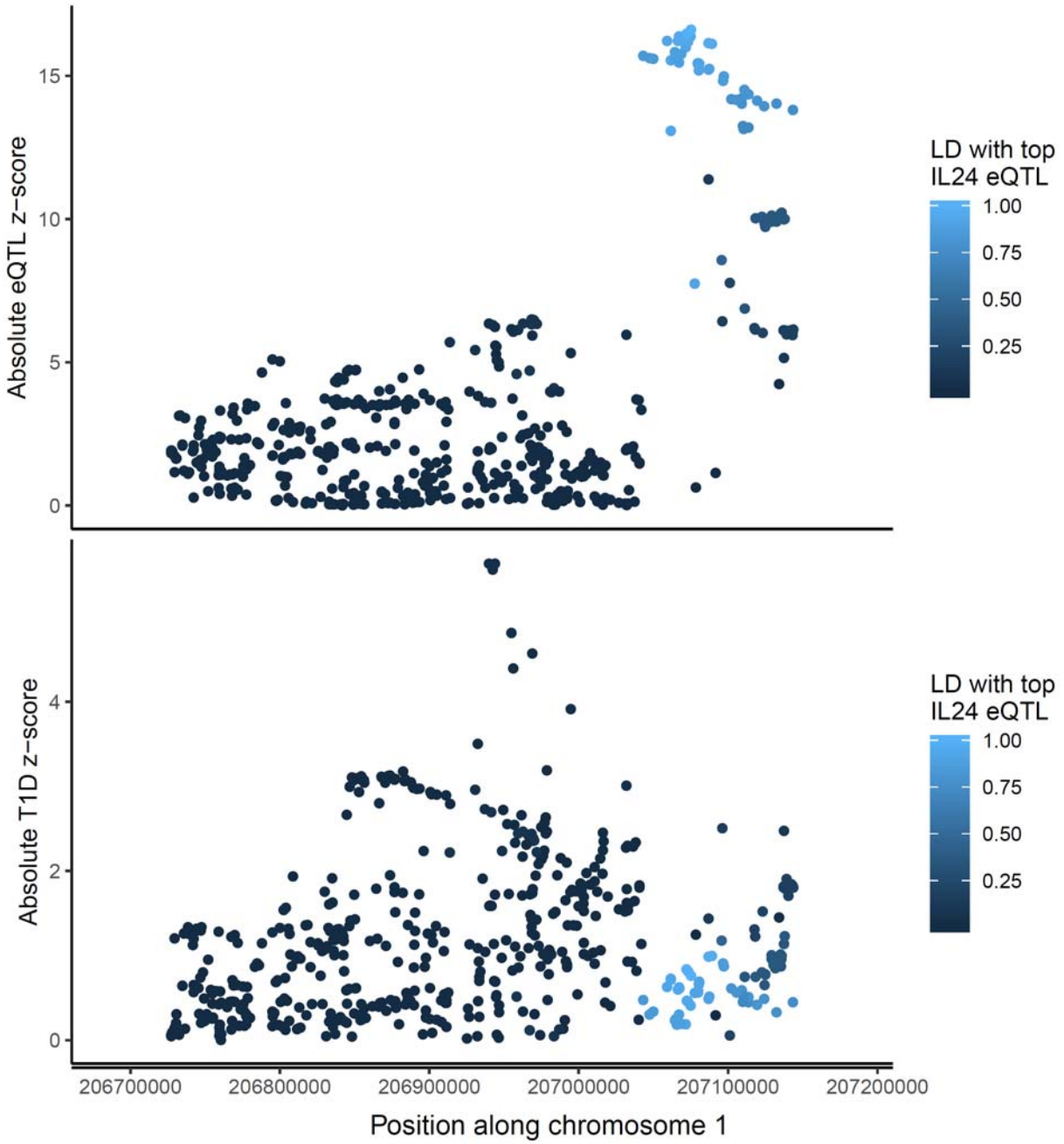

SUPPLEMENTARY DATA

**Supplementary Figure 16.** Top panel: association absolute z-scores from whole blood eQTL study examining variant effects on FAIM3 mRNA levels, coloured by LD $r^2$ to the most strongly associated variant with FAIM3 mRNA expression. Bottom panel: association absolute z scores from logistic regression examining variant associations with type 1 diabetes risk diagnosed at <7 years, using individuals from the UK and Northern Ireland only and adjusting for the five largest principal components as derived from genotype data, coloured by LD $r^2$ to the most strongly associated variant with FAIM3 mRNA. Shows most associated disease risk variants are not in high LD with the most associated FAIM3 whole blood eQTLs.

SUPPLEMENTARY DATA

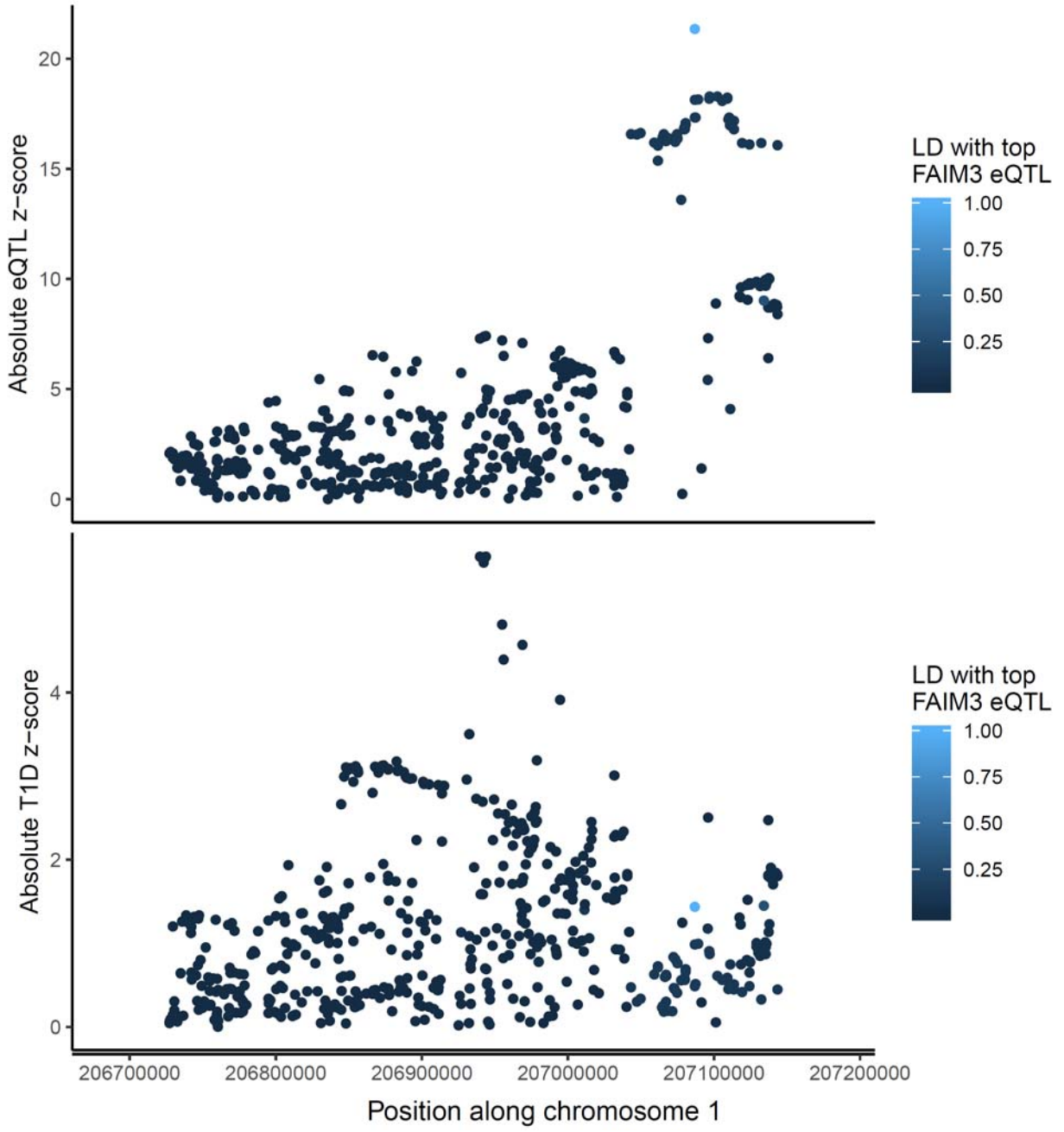

SUPPLEMENTARY DATA

**Supplementary Material**

## Approaches

### Study populations

The individuals were recruited into various collections, UK-based individuals from the type 1 diabetes genetics consortium (T1DGC) [1], the genetic resource investigating diabetes (GRID), the Warren cohort [2], the northern Irish GRID [3], the 1958 birth control cohort and the UK blood service [1], individuals from central Europe, Asia-Pacific and the USA from the T1DGC and individuals from Finland from the IDDMGEN and T1DGEN cohorts [4]. One of the inclusion criteria in the GRID cohort was diagnosis at ≤16 years, strongly suggesting these individuals have type 1 diabetes. For the T1DGC families, the age-at-diagnosis cut off was higher at 35 years but the cases needed to have started insulin within 6 months of diagnosis and stayed continuously on insulin without stopping for 6 or more months, suggesting genuine type 1 diabetes as opposed to type 2 diabetes.

When sex data was missing for samples, we imputed this data based on the homozygosity rate on the X chromosome. Individuals with homozygosity rates between 0.65 and 0.85 were assumed female and individuals with homozygosity rates greater than 0.93 were assumed male.

### Genotyping and quality control

All samples were genotyped using the Illumina ImmunoChip [1], a specialised platform which densely genotypes regions of interest for autoimmune diseases. Quality control was performed by excluding variants with a minor allele frequency <0.01, a Hardy-Weinberg equilibrium exact test p value of $<5\times10^{-4}$ or greater than 5% missing values. Eleven T1D-associated variants we examined failed such quality control and were therefore imputed for analysis.

### Relatedness calculations

We grouped the individuals into three groups, individuals from the UK, individuals from Finland and individuals recruited into the T1DGC study. From each group, we removed those related to closer than second degree by pruning variants correlated to $r^2$ >0.2 and removing the major histocompatility (MHC) region, then calculating relatedness using the KING 2.0.9 software [5], leaving the total of 27,071 individuals for analysis. After removing variants in linkage disequilibrium (LD) and the MHC region (chromosome 6, positions 25000000-35000000 genome build 36), 28,208 variants were used for relationship inference in the UK group, 28,280 in the T1DGC group and 26,586 in the Finnish group.

### Type 2 diabetes genetic risk score (GRS)

In order to increase confidence that no individuals in the ≥13 group had type 2 diabetes, we took 30 variants associated with type 2 diabetes and their corresponding log-odds ratios for type 2 diabetes [6]. For each individual in the analysis, we multiplied the number of risk variants by the type 2 diabetes log-odds ratio and summed these together over the 30 loci to generate a type 2 diabetes GRS.

### Principal components analysis

The top 10 genetic principal components were adjusted for in each analysis and were generated using ImmunoChip data filtered so that a set of independent variants ($r^2$<0.2) were kept and the MHC region was excluded entirely (chromosome 6, positions 25000000-35000000 genome build 36), leaving a total of 24,452 variants for which to calculate principal components from. The PLINK software was used to carry out this procedure [7]. For the UK-specific sensitivity analyses and fine-mapping analyses, the five largest principal components were used as calculated using UK-ancestry individuals only, since there was very little population structure expected and observed in this population.

### False discovery rate

The false discovery rate used throughout this manuscript is the Benjamini-Hochberg false discovery rate [8].

### Binomial test examining variants not associated to FDR <0.1

Given there are three AAD groups in our analysis, there are six possible ways the log-odds ratio

estimates could be ordered. If there were to be no differences in genetic effect between AAD groups, we would expect approximately one sixth of the variants tested to be in each of the possible orders. We therefore performed a binomial test comparing the number of times the ordering was the largest effect estimate in the <7s, the intermediate effect estimate in the 7-13s and the smallest effect estimate in the ≥13s to that expected by chance (1/6=0.167).

**Fine-mapping**

To guard against identifying false positive associations due to imputation, we removed variants from the stochastic search that had a certainty call rate of <75%, a minor allele frequency of <0.005, an absolute Hardy-Weinberg equilibrium z score of >8 (in controls only) and a variant imputation information score of <0.8. We also excluded variants with a difference in imputation information score between cases and controls of more than 0.01, a concordance rate between genotypes and imputed genotype call of <0.8 or where the ratio of the variance to approximate expected variance for a variant with that minor allele frequency (MAF) (≈2×MAF×(1-MAF)) was greater than 0.05.

We adjusted for sex and the five largest genetic principal components calculated from UK individuals genotype data, set the prior mean number of expected causal variants in the region to be three and saved the top 10,000 most visited models for downstream analysis.

**Colocalisation analyses**

Summary statistics from both association studies (disease risk and eQTL) were converted to approximate Bayes Factors (ABFs). Posterior probabilities were then calculated for each of the following scenarios: i) association with disease only, ii) association with eQTL only, iii) association with disease and eQTL but distinct signals or iv) shared disease and eQTL signal in the region [9]. We focus on scenario iv), colocalisation of disease and eQTL signal, which is calculated by multiplying the ABFs for disease and eQTL together for each variant (to get the likelihood of colocalisation) and multiplying this by the prior probability of colocalisation, which we took to be $1\times10^{-5}$, reflecting a prior belief that 1 variant in every 10 that is associated with type 1 diabetes will also be associated with the eQTL (since the prior probability of association for disease and eQTL was taken to be $1\times10^{-4}$). Dividing this product by the normalising factor, the overall probability of all combinations of each of the four hypotheses and also the probability of no association with disease or eQTL, gives the posterior probability of colocalisation.

SUPPLEMENTARY DATA

**Supplementary Table 1.** Classical HLA alleles/haplotypes examined in analysis.

| Haplotype/allele name | Haplotype/allele definition | Individuals included | Conditioned on | Enough individuals to include? |
|---|---|---|---|---|
| DR3-DQ2 | DRB1*03:01-DQB1*02:01 | Non-DR3/4 only | Sex, 5 PCs, A*02:01, A*24:02, B*39:06, B*18:01 | Yes |
| DR4-DQ8 | DRB1*04:01-DQB1*03:02<br>DRB1*04:02-DQB1*03:02<br>DRB1*04:04-DQB1*03:02<br>DRB1*04:05-DQB1*03:02<br>DRB1*04:08-DQB1*03:02<br>DRB1*04:01-DQB1*03:04<br>DRB1*04:02-DQB1*03:04<br>DRB1*04:04-DQB1*03:04<br>DRB1*04:05-DQB1*03:04<br>DRB1*04:08-DQB1*03:04<br>DRB1*04:01-DQB1*02:02<br>DRB1*04:02-DQB1*02:02<br>DRB1*04:04-DQB1*02:02<br>DRB1*04:05-DQB1*02:02<br>DRB1*04:08-DQB1*02:02 | Non-DR3/4 only | Sex, 5 PCs, A*02:01, A*24:02, B*39:06, B*18:01. | Yes |
| DR3-DQ2/DR4-DQ8 | Any combination of rows 1 and 2 above, one on either chromosome. | All individuals | Sex, 5 PCs, A*02:01, A*24:02, B*39:06, B*18:01. | Yes |
| DRB1*13:03-DQB1*03:01 | DRB1*13:03-DQB1*03:01 | Non-DR3/4 only | Sex, 5 PCs. | No |
| DRB1*11:04-DQB1*03:01 | DRB1*11:04-DQB1*03:01 | Non-DR3/4 only | Sex, 5 PCs. | No |
| DRB1*15:01-DQB1*06:02 | DRB1*15:01-DQB1*06:02 | Non-DR3/4 only | Sex, 5 PCs. | Yes |
| DRB1*07:01-DQB1*03:03 | DRB1*07:01-DQB1*03:03 | Non-DR3/4 only | Sex, 5 PCs. | Yes |
| DRB1*14:01-DQB1*05:03 | DRB1*14:01-DQB1*05:03 | Non-DR3/4 only | Sex, 5 PCs. | No |
| A*02:01 | A*02:01 | All individuals | Sex, 5 PCs, DR3-DQ2, DR4-DQ8, DR3-DQ2/DR4-DQ8, B*39:06 | Yes |
| A*24:02 | A*24:02 | All individuals | Sex, 5 PCs, DR3-DQ2, DR4-DQ8, DR3-DQ2/DR4-DQ8, B*39:06 | Yes |
| A*11:01 | A*11:01 | All individuals | Sex, 5 PCs, DR3-DQ2, DR4-DQ8, DR3-DQ2/DR4-DQ8, B*39:06 | Yes |
| A*32:01 | A*32:01 | All individuals | Sex, 5 PCs, DR3-DQ2, DR4-DQ8, DR3-DQ2/DR4-DQ8, B*39:06 | Yes |
| DPB1*03:01 | DPB1*03:01 | All individuals | Sex, 5 PCs, DR3-DQ2, DR4-DQ8, DR3-DQ2/DR4-DQ8, A24*02, B*39:06 | Yes |
| DPB1*04:02 | DPB1*04:02 | All individuals | Sex, 5 PCs, DR3-DQ2, DR4-DQ8, DR3-DQ2/DR4-DQ8, A24*02, B*39:06 | Yes |
| B*18:01 | B*18:01 | All individuals | Sex, 5 PCs, DR3-DQ2, DR4-DQ8, DR3-DQ2/DR4-DQ8, A24*02 | Yes |
| B*39:06 | B*39:06 | All individuals | Sex, 5 PCs, DR3-DQ2, DR4-DQ8, DR3-DQ2/DR4-DQ8, A24*02, | Yes |
| B*44:03 | B*44:03 | All individuals | Sex, 5 PCs, DR3-DQ2, DR4-DQ8, DR3-DQ2/DR4-DQ8, A24*02, | Yes |

SUPPLEMENTARY DATA

**Supplementary Table 2.** Non-HLA variants examined in analysis.

| Variant name | Chr | Position (genome build 37) | Publication(s) where association identified* | Locus name in Figures in this manuscript |
|---|---|---|---|---|
| rs2476601 | 1 | 114377568 | Onengut-Gumuscu | *PTPN22* |
| rs78037977 | 1 | 172681031 | Fortune | *TNFSF4*** |
| rs6691977 | 1 | 200814959 | Onengut-Gumuscu | *CAMSAP2* |
| rs3024505 | 1 | 206939904 | Onengut-Gumuscu | *IL10* |
| rs4849135 | 1 | 111615079 | Onengut-Gumuscu | *ACOXL* |
| rs13415583 | 2 | 100764087 | Onengut-Gumuscu | *AFF3* |
| rs2111485 | 2 | 163110536 | Onengut-Gumuscu | *IFIH1 (1)* |
| rs35667974 | 2 | 163124637 | Onengut-Gumuscu | *IFIH1 (2)* |
| rs72871627 | 2 | 163136942 | Onengut-Gumuscu | *IFIH1 (3)* |
| rs3087243 | 2 | 204738919 | Onengut-Gumuscu | *CTLA4* |
| rs113010081 | 3 | 46457412 | Onengut-Gumuscu | *CCR5* |
| rs6819058 | 4 | 123114622 | Burren | *IL2/IL21 (1)* |
| rs67797421 | 4 | 123116177 | Burren | *IL2/IL21 (2)* |
| rs2611215 | 4 | 166574267 | Onengut-Gumuscu | *CPE* |
| rs11954020 | 5 | 35883251 | Onengut-Gumuscu | *IL7R* |
| rs72975913 | 6 | 128293932 | Inshaw | *THEMIS* |
| rs72928038 | 6 | 90976768 | Onengut-Gumuscu | *BACH2* |
| rs1538171 | 6 | 126752884 | Onengut-Gumuscu | *CENPW* |
| rs62447205 | 7 | 50465830 | Onengut-Gumuscu | *IKZF1* |
| rs10277986 | 7 | 51028987 | Onengut-Gumuscu | *COBL* |
| rs6476839 | 9 | 4290823 | Onengut-Gumuscu | *GLIS3* |
| rs61839660 | 10 | 6094697 | Wallace | *IL2RA (1)* |
| rs11594656 | 10 | 6122009 | Wallace | *IL2RA (2)* |
| rs6602437 | 10 | 6130077 | Wallace | *IL2RA (3)* |
| rs41295121 | 10 | 6129643 | Wallace | *IL2RA (4)* |
| rs12416116 | 10 | 90035654 | Onengut-Gumuscu | *PTEN*** |
| rs689 | 11 | 2182224 | Onengut-Gumuscu | *INS (1)* |
| rs72853903 | 11 | 2198665 | Onengut-Gumuscu | *INS (2)* |
| rs917911 | 12 | 9905851 | Onengut-Gumuscu | *CD69* |
| rs705705 | 12 | 56435504 | Onengut-Gumuscu | *IKZF4* |
| rs653178 | 12 | 112007756 | Onengut-Gumuscu | *SH2B3* |
| rs9585056 | 13 | 100081766 | Onengut-Gumuscu | *GPR183* |
| rs1456988 | 14 | 98488007 | Onengut-Gumuscu | *LINC01550* |
| rs56994090 | 14 | 101306447 | Onengut-Gumuscu | *MEG3* |
| rs72727394 | 15 | 38847022 | Onengut-Gumuscu | *RASGRP1* |
| rs34593439 | 15 | 79234957 | Onengut-Gumuscu | *CTSH* |
| rs151234 | 16 | 28505660 | Onengut-Gumuscu | *IL27* |
| rs12927355 | 16 | 11194771 | Onengut-Gumuscu | *DEXI (1)* |
| rs193778 | 16 | 11351211 | Onengut-Gumuscu | *DEXI (2)* |
| rs8056814 | 16 | 75252327 | Onengut-Gumuscu | *CTRB1*** |
| rs12453507 | 17 | 38053207 | Onengut-Gumuscu | *IKZF3* |
| rs757411 | 17 | 38775150 | Onengut-Gumuscu | *CCR7* |
| rs1052553 | 17 | 44073889 | Onengut-Gumuscu | *MAPT* |
| rs1893217 | 18 | 12809340 | Onengut-Gumuscu | *PTPN2 (1)* |
| rs12971201 | 18 | 12830538 | Onengut-Gumuscu | *PTPN2 (2)* |
| rs1615504 | 18 | 67526644 | Onengut-Gumuscu | *CD226* |
| rs34536443 | 19 | 10463118 | Onengut-Gumuscu | *TYK2 (1)* |

SUPPLEMENTARY DATA

| | | | | |
|---|---|---|---|---|
| rs12720356 | 19 | 10469975 | Onengut-Gumuscu | *TYK2 (2)* |
| rs402072 | 19 | 47219122 | Onengut-Gumuscu | *PRKD2* |
| rs516246 | 19 | 49206172 | Onengut-Gumuscu | *FUT2* |
| rs6043409 | 20 | 1616206 | Onengut-Gumuscu | *SIRPG* |
| rs11203202 | 21 | 43825357 | Onengut-Gumuscu | *UBASH3A* |
| rs6518350 | 21 | 45621817 | Onengut-Gumuscu | *ICOSLG* |
| rs4820830 | 22 | 30531091 | Onengut-Gumuscu | *HORMAD2* |
| rs229533 | 22 | 37587111 | Onengut-Gumuscu | *C1QTNF6* |

*Most recent publication listed. Onengut-Gumuscu [1], Fortune [10], Burren [11], Inshaw [3], Wallace [12].
**Candidate gene different from previous reports based on publically available gene expression (https://dice-database.org/) and promoter-capture Hi-C data (https://www.chicp.org).

SUPPLEMENTARY DATA

**Supplementary Table 3.** Non-HLA region variants with evidence of heterogeneity in effect size between the <7 and ≥13 groups: Promoter Capture Hi-C (PCHi-C) candidate genes.

| **Locus name/ karyotype band** | **Tag/index variant** | **Candidate causal genes** | **PCHi-C prioritised protein coding genes*** | **PCHi-C prioritised non-protein coding transcripts** |
|---|---|---|---|---|
| *CTSH* / 15q25.1 | rs34593439 | *CTSH* | *CTSH*<br>*BCL2A1* | - |
| *GLIS3* / 9p24.2 | rs6476839 | *GLIS3* | *GLIS3*** | *GLIS3-AS1*** |
| *IKZF3* / 17q21 | rs12453507 | *IKZF3*<br>*ORMDL3*<br>*GSDMB* | *ORMDL3*<br>*GSDMB*<br>*ZPBP2* | - |
| *IL2RA* (3) / 10p15.1 | rs6602437 | *IL2RA* | *RBM17*<br>*IL2RA*<br>*GDI2*<br>*PRKCQ*<br>*ANKRD16*<br>*FAM208B*<br>*FBX018* | *RP11-536K7.3*<br>*PRKCQ-AS1* |
| *THEMIS* / 6q22.33 | rs72975913 | *PTPRK*<br>*THEMIS* | *PTPRK*<br>*THEMIS* | |
| *IL10 /* 1q32.1 | rs3024505 | *IL10*<br>*FAIM3* | *IL10*<br>*FCAMR*<br>*IL20*<br>*FAIM3*<br>*PIGR*<br>*CD55*<br>*IL24*<br>*IL19* | - |

*Inshaw et. al [13]
** Miguel-Escalada et al. [14]

SUPPLEMENTARY DATA

**Supplementary Table 4.** Details of non-HLA variants with evidence of heterogeneity in effect size between the <7 and ≥13 groups.

| Locus name/ karyotype band | Tag/index variant | Candidate causal genes | Tissues expressed* | BLUEPRINT [15] / DICE** database immune cell types expressed*** | Function |
|---|---|---|---|---|---|
| *CTSH* / 15q25.1 | rs34593439 | *CTSH* | Ubiquitous | Macrophages, DCs, T and B cells, monocytes | CTSH is a lysosomal protein, has amino- and endopeptidase activity [16] and has the potential to generate hybrid peptides [17]. CTSH has been reported to process pro-surfactant protein B [18] and pro-granzyme B [19] into their active mature forms. Proteolytic cleavage of TLR3 by CTSH alters the stability, localization and/or the regulation of TLR3 activity [20, 21]. CTSH-deficient mice have reduced TLR3 expression and type 1 IFN release in response to poly(I:C) stimulation [22] and T1D associated SNPs colocalise with a monocyte eQTL signal [23]. |
| *GLIS3* / 9p24.2 | rs6476839 | *GLIS3* | Pancreas, thyroid gland, kidney, ovary | - | GLIS3 is a transcriptional regulator [24], required for insulin expression [25], function and transcriptional program of mature □eta cells [26]. A key molecule regulating the response to unfolded protein stress and protection of □eta cells from apoptosis [27, 26]. |
| *IKZF3* / 17q21 | rs12453507 | *IKZF3*<br>*ORMDL3*<br>*GSDMB* | *IKZF3*: Small intestine, spleen<br><br>*ORMDL3*: Ubiquitous<br><br>*GSDMB*: Ubiquitous | *IKZF3*: thymocytes, B, T and NK cells<br><br>*ORMDL3*: thymocytes, T, B, and NK cells, eosinophils<br><br>*GSDMB*: thymocytes, T, B and NK cells, eosinophils | *IKZF3 (Ailos)*: A transcriptional regulator and a member of the Ikaros gene family [28]. IKZF3 regulates B cell activation thresholds and differentiation [29] and is required for generation of high affinity plasma cells [30].<br>In T cells, IKZF3 acts as a transcriptional repressor to promote Th17 differentiation [31] and can modulate the activity of FoxP3 [32].<br><br>*ORMDL3*: regulates sphingolipid biosynthesis and expression is increased by inflammatory stimuli [33]. ORMDL3 is a negative regulator of store operated calcium entry [34] and modulates lymphocyte activation and cytokine production [35].<br><br>*GSDMB*: GSDMB can be cleaved by apoptotic caspases [36] and the active form of GSDMB induces pyroptotic cell death in epithelial cells [37]. |
| *IL2RA* (3) / 10p15.1 | rs6602437 | *IL2RA* | Bone marrow, Lymph nodes, spleen | Thymocytes, T, B, NK | *IL2RA* encodes CD25 the alpha chain of the trimeric high affinity IL-2 receptor. IL-2 signaling controls T cell growth and differentiation, NK cell |

SUPPLEMENTARY DATA

| | | | | | |
|---|---|---|---|---|---|
| | | | | | and activated B cell proliferation and is essential for the survival and function of regulatory T cells (Tregs) [38, 39] |
| *THEMIS* / 6q22.33 | rs72975913 | *PTPRK* *THEMIS* | *PTPRK*: Ubiquitous<br><br>*THEMIS*: Spleen, small intestine, thymus | *PTPRK*: Thymocytes, naïve T cells, B cells<br><br>*THEMIS*: Thymocytes, T cells | *PTPRK*: Protein tyrosine phosphatase receptor type kappa may be involved in thymic selection of single positive CD4 T cells [40].<br><br>*THEMIS*: Thymocyte-expressed molecule involved in selection regulates phosphatase activity (Shp1) in developing thymocytes to enable positive selection [41, 42]. In peripheral T cells, dependent upon intracellular interacting partners, Themis alters T cell signalling to positively [43] or negatively [44] control T cell activation through the TCR. |
| *IL10* / 1q32.1 | rs3024505 | *IL10* *FAIM3* | *IL10:* Spleen<br><br>*FAIM3:* Spleen, small intestine | *IL10*: Monocytes, activated T, Treg, macrophages and B cells.<br><br>*FAIM3*: T and B cells | *IL10*: Interleukin 10 is a key cytokine that modulates immune and non-immune cell function [45]. IL10 can be produced by specialized regulatory T [46] and B cell populations [47].<br>Primary mechanisms include downregulation of MHC class II and cytokine responses of antigen-presenting cells [48] and induction of anergy in T cells [49]. IL10 acts as a potent growth and differentiation factor for B cells [50].<br><br>*FAIM3:* Encodes FCmR a receptor for natural IgM [51] and involved in B cell homeostasis [52], control of IL10 production [53] and supports early B cell activation events and plasma cell development [54]. |

*Human protein atlas: https://www.proteinatlas.org
** DICE database: https://dice-database.org/
*** T=T cells, B= B cells, NK = Natural Killer cells, DC= Dendritic cells.

***INCLUDE***:
(i) candidate genes nominated in Onengut-Gumuscu et al [1] and Inshaw et al [13].
(ii) genes prioritised by promoter capture Hi-C (PCHi-C) in immune cells [13, 55], or gene promoter interactions with credible SNPs in islet PCHi-C [14].

***FILTER ON***:
(i) expression in immune cells (https://dice-database.org/) or islets [56]
***and/or***
(ii) eQTL in whole blood [57] passing a Bonferroni corrected p value threshold ($p < 2.78 \times 10^{-13}$).

SUPPLEMENTARY DATA

**Supplementary Table 5.** Most likely variants causally associated with T1D at the *CTSH* locus from GUESSFM fine mapping analysis.

| Variant | Position (gr37) | Log-odds ratio | Reference allele | Effect allele | Variant posterior probability | Group posterior probability |
|---|---|---|---|---|---|---|
| rs12592898 | 79229199 | -0.2687 | G | A | 1.13e-02 | 1 |
| rs60254670 | 79229959 | -0.2613 | TGGCCAGAATG | T | 5.43e-03 | 1 |
| rs12148472 | 79231478 | -0.2723 | T | C | 2.13e-02 | 1 |
| rs34843303 | 79234470 | -0.3248 | T | C | 3.58e-01 | 1 |
| rs34593439 | 79234957 | -0.3315 | G | A | 3.34e-01 | 1 |
| rs2289702 | 79237293 | -0.3403 | C | T | 2.70e-01 | 1 |

SUPPLEMENTARY DATA

**Supplementary Table 6.** Most likely variants causally associated with T1D at the *GLIS3* locus from GUESSFM fine mapping analysis.

| Variant | Position (gr37) | Log-odds ratio | Reference allele | Effect allele | Variant posterior probability | Group posterior probability |
|---|---|---|---|---|---|---|
| rs4380994 | 4282536 | -0.1392 | A | G | 3.58e-02 | 0.9844 |
| rs3892354 | 4282942 | -0.1373 | T | G | 2.45e-02 | 0.9844 |
| rs1574285 | 4283137 | -0.1304 | G | T | 7.70e-03 | 0.9844 |
| rs10974435 | 4283682 | -0.1417 | T | C | 5.28e-02 | 0.9844 |
| rs34494309 | 4284961 | -0.1368 | A | AT | 2.34e-02 | 0.9844 |
| rs57884925 | 4285119 | -0.1378 | G | C | 2.79e-02 | 0.9844 |
| rs10758591 | 4285986 | -0.1421 | G | C | 5.44e-02 | 0.9844 |
| rs7024686 | 4287211 | -0.1426 | G | C | 6.17e-02 | 0.9844 |
| rs7041847 | 4287466 | -0.1395 | A | G | 3.64e-02 | 0.9844 |
| rs7034200 | 4289050 | -0.1392 | A | C | 3.60e-02 | 0.9844 |
| rs10814914 | 4289196 | -0.1424 | T | C | 6.20e-02 | 0.9844 |
| rs10116772 | 4290541 | -0.133 | A | C | 1.10e-02 | 0.9844 |
| rs10814915 | 4290544 | -0.1399 | T | C | 3.66e-02 | 0.9844 |
| rs6476839 | 4290823 | -0.1397 | T | A | 3.15e-02 | 0.9844 |
| rs6476842 | 4291268 | -0.142 | C | T | 5.33e-02 | 0.9844 |
| rs7020673 | 4291747 | -0.1406 | G | C | 4.09e-02 | 0.9844 |
| rs10974438 | 4291928 | -0.1452 | C | A | 4.71e-02 | 0.9844 |
| rs10758593 | 4292083 | -0.138 | A | G | 2.37e-02 | 0.9844 |
| rs7867224 | 4292152 | -0.1426 | A | G | 6.09e-02 | 0.9844 |
| rs10814916 | 4293150 | -0.1403 | C | A | 4.23e-02 | 0.9844 |
| rs34706136 | 4294707 | -0.1455 | TG | T | 4.32e-02 | 0.9844 |
| rs10758594 | 4295583 | -0.1453 | A | G | 8.99e-02 | 0.9844 |
| rs4339696 | 4295880 | -0.1302 | G | T | 8.48e-03 | 0.9844 |
| rs10814917 | 4296430 | -0.1437 | A | G | 7.30e-02 | 0.9844 |

SUPPLEMENTARY DATA

**Supplementary Table 7.** Most likely variants causally associated with T1D at the *IKZF3* locus from GUESSFM fine mapping analysis.

| Variant | Position (gr37) | Log-odds ratio | Reference allele | Effect allele | Variant posterior probability | Group posterior probability |
|---|---|---|---|---|---|---|
| rs2941522 | 37910368 | -0.1772 | C | T | 2.67e-02 | 0.9819 |
| rs12946510 | 37912377 | -0.153 | T | C | 6.66e-04 | 0.9819 |
| rs72538185 | 37916390 | -0.178 | A | AT | 2.93e-02 | 0.9819 |
| rs907091 | 37921742 | -0.1796 | C | T | 4.64e-02 | 0.9819 |
| rs907092 | 37922259 | -0.155 | A | G | 8.94e-04 | 0.9819 |
| rs2952140 | 37928059 | -0.1801 | C | T | 5.22e-02 | 0.9819 |
| rs2313430 | 37929816 | -0.1813 | T | C | 6.59e-02 | 0.9819 |
| rs10445308 | 37938047 | -0.1527 | T | C | 6.80e-04 | 0.9819 |
| rs12942330 | 37939839 | -0.1517 | T | C | 5.84e-04 | 0.9819 |
| rs11658993 | 37940808 | -0.1524 | T | C | 6.42e-04 | 0.9819 |
| rs2952144 | 37960017 | -0.1762 | C | T | 2.37e-02 | 0.9819 |
| rs4795395 | 37962987 | -0.1511 | A | T | 5.28e-04 | 0.9819 |
| rs9909593 | 37970149 | -0.1522 | G | A | 6.20e-04 | 0.9819 |
| rs71152606 | 37975214 | -0.1769 | CTTCTA | C | 2.35e-02 | 0.9819 |
| rs9303277 | 37976469 | -0.1765 | T | C | 2.51e-02 | 0.9819 |
| rs3816470 | 37985801 | -0.1725 | G | A | 1.05e-02 | 0.9819 |
| rs4795397 | 38023745 | -0.1487 | G | A | 3.31e-04 | 0.9819 |
| rs11557466 | 38024626 | -0.157 | T | C | 1.53e-03 | 0.9819 |
| rs11078925 | 38025208 | -0.1572 | C | T | 1.65e-03 | 0.9819 |
| rs34120102 | 38026035 | -0.1578 | A | G | 1.84e-03 | 0.9819 |
| rs11655198 | 38026169 | -0.1786 | T | C | 3.73e-02 | 0.9819 |
| rs11650661 | 38026286 | -0.1787 | T | A | 3.79e-02 | 0.9819 |
| rs11655292 | 38026361 | -0.1788 | G | C | 3.86e-02 | 0.9819 |
| rs12709365 | 38027400 | -0.1571 | G | A | 1.53e-03 | 0.9819 |
| rs13380815 | 38027583 | -0.1563 | G | A | 1.36e-03 | 0.9819 |
| rs11557467 | 38028634 | -0.1795 | T | G | 4.26e-02 | 0.9819 |
| rs12936231 | 38029120 | -0.1795 | G | C | 4.35e-02 | 0.9819 |
| rs11870965 | 38030205 | -0.1565 | A | T | 1.39e-03 | 0.9819 |
| rs9903250 | 38031030 | -0.1791 | A | G | 4.04e-02 | 0.9819 |
| rs9905959 | 38031138 | -0.1555 | G | A | 1.07e-03 | 0.9819 |
| rs11658278 | 38031164 | -0.1786 | C | T | 3.35e-02 | 0.9819 |
| rs10852935 | 38031674 | -0.1582 | T | C | 1.89e-03 | 0.9819 |
| rs10852936 | 38031714 | -0.1571 | T | C | 1.53e-03 | 0.9819 |
| rs9891174 | 38031802 | -0.1555 | A | T | 1.15e-03 | 0.9819 |
| rs59716545 | 38031857 | -0.1582 | G | T | 1.91e-03 | 0.9819 |
| rs36095411 | 38031865 | -0.1721 | G | T | 7.51e-03 | 0.9819 |
| rs12939457 | 38032188 | -0.1553 | C | T | 1.05e-03 | 0.9819 |
| rs367998020 | 38032200 | -0.1553 | A | AGTGCAGT | 1.05e-03 | 0.9819 |
| rs34189114 | 38032460 | -0.158 | T | C | 1.91e-03 | 0.9819 |
| rs35736272 | 38032680 | -0.1583 | C | T | 1.94e-03 | 0.9819 |
| rs1054609 | 38033277 | -0.1576 | C | A | 1.68e-03 | 0.9819 |
| rs9907088 | 38035116 | -0.1575 | A | G | 1.68e-03 | 0.9819 |
| rs36038753 | 38035370 | -0.1601 | T | G | 2.57e-03 | 0.9819 |
| rs35569035 | 38035624 | -0.1582 | T | C | 1.91e-03 | 0.9819 |
| rs9910826 | 38035648 | -0.1559 | G | A | 1.26e-03 | 0.9819 |
| rs71355426 | 38035766 | -0.1564 | G | GAGA | 1.40e-03 | 0.9819 |
| rs9904624 | 38036586 | -0.1554 | G | A | 1.16e-03 | 0.9819 |
| rs4795398 | 38038179 | -0.1548 | T | C | 1.05e-03 | 0.9819 |
| rs12939565 | 38038389 | -0.1772 | T | A | 2.80e-02 | 0.9819 |
| rs12939566 | 38038390 | -0.1543 | T | A | 9.44e-04 | 0.9819 |

| | | | | | | |
|---|---|---|---|---|---|---|
| rs71152620 | 38039561 | -0.1757 | T | TAACA | 2.11e-02 | 0.9819 |
| rs12232497 | 38040119 | -0.1558 | C | T | 1.21e-03 | 0.9819 |
| rs12232498 | 38040363 | -0.1533 | C | T | 7.88e-04 | 0.9819 |
| rs12941333 | 38040534 | -0.1533 | T | C | 7.85e-04 | 0.9819 |
| rs2872507 | 38040763 | -0.1547 | A | G | 9.96e-04 | 0.9819 |
| rs9908132 | 38042777 | -0.1746 | A | T | 1.70e-02 | 0.9819 |
| rs9901146 | 38043343 | -0.1748 | A | G | 1.70e-02 | 0.9819 |
| rs12936409 | 38043649 | -0.1547 | T | C | 1.01e-03 | 0.9819 |
| rs12103884 | 38045725 | -0.1755 | T | C | 1.94e-02 | 0.9819 |
| rs9906951 | 38048244 | -0.1759 | C | T | 2.18e-02 | 0.9819 |
| rs12950209 | 38049102 | -0.1746 | C | T | 1.72e-02 | 0.9819 |
| rs12950743 | 38049233 | -0.1751 | C | T | 1.83e-02 | 0.9819 |
| rs7359623 | 38049589 | -0.1614 | T | C | 1.40e-03 | 0.9819 |
| rs68122720 | 38050092 | -0.153 | A | AAG | 7.32e-04 | 0.9819 |
| rs8067378 | 38051348 | -0.1764 | G | A | 2.32e-02 | 0.9819 |
| rs12453507 | 38053207 | -0.1662 | G | C | 3.57e-03 | 0.9819 |
| rs34170568 | 38055921 | -0.154 | ATT | A | 5.19e-04 | 0.9819 |
| rs11651596 | 38056116 | -0.1481 | C | T | 2.82e-04 | 0.9819 |
| rs12949100 | 38057189 | -0.1501 | A | G | 4.14e-04 | 0.9819 |
| rs8069176 | 38057197 | -0.1494 | A | G | 3.61e-04 | 0.9819 |
| rs4795399 | 38061439 | -0.1509 | C | T | 4.70e-04 | 0.9819 |
| rs2305480 | 38062196 | -0.1509 | A | G | 4.70e-04 | 0.9819 |
| rs2305479 | 38062217 | -0.1715 | T | C | 9.61e-03 | 0.9819 |
| rs35196450 | 38062942 | -0.1503 | AC | A | 4.11e-04 | 0.9819 |
| rs56750287 | 38062944 | -0.1504 | C | A | 4.21e-04 | 0.9819 |
| rs11078926 | 38062976 | -0.1509 | A | G | 4.70e-04 | 0.9819 |
| rs883770 | 38063381 | -0.1706 | T | C | 8.17e-03 | 0.9819 |
| rs62067034 | 38063738 | -0.1727 | T | C | 1.23e-02 | 0.9819 |
| rs36000226 | 38063929 | -0.1725 | C | T | 1.18e-02 | 0.9819 |
| rs36084703 | 38063980 | -0.1734 | C | CA | 1.43e-02 | 0.9819 |
| rs11078927 | 38064405 | -0.1508 | T | C | 4.61e-04 | 0.9819 |
| rs11078928 | 38064469 | -0.1503 | C | T | 4.30e-04 | 0.9819 |
| rs12939832 | 38064876 | -0.1501 | A | G | 3.24e-04 | 0.9819 |
| rs2290400 | 38066240 | -0.1736 | C | T | 1.44e-02 | 0.9819 |
| rs1008723 | 38066267 | -0.1714 | T | G | 9.58e-03 | 0.9819 |
| rs4795400 | 38067020 | -0.1477 | T | C | 2.64e-04 | 0.9819 |
| rs869402 | 38068043 | -0.1668 | T | C | 3.84e-03 | 0.9819 |
| rs1011082 | 38068514 | -0.1656 | T | C | 2.99e-03 | 0.9819 |
| rs921650 | 38069076 | -0.1675 | G | A | 4.38e-03 | 0.9819 |
| rs921649 | 38069274 | -0.1669 | C | T | 4.08e-03 | 0.9819 |
| rs6503524 | 38069809 | -0.1667 | C | T | 3.89e-03 | 0.9819 |
| rs7216389 | 38069949 | -0.1667 | C | T | 3.85e-03 | 0.9819 |
| rs7216558 | 38070071 | -0.169 | C | T | 5.87e-03 | 0.9819 |
| rs150597688 | 38071086 | -0.1684 | C | CTT | 5.15e-03 | 0.9819 |
| rs143385463 | 38071855 | -0.1655 | ATTT | A | 3.32e-03 | 0.9819 |
| rs1031458 | 38072173 | -0.1674 | G | T | 4.38e-03 | 0.9819 |
| rs1031460 | 38072247 | -0.171 | T | G | 9.06e-03 | 0.9819 |
| rs8065777 | 38072402 | -0.1681 | C | T | 5.11e-03 | 0.9819 |
| rs7219923 | 38074518 | -0.1674 | C | T | 4.46e-03 | 0.9819 |
| rs7224129 | 38075426 | -0.1671 | G | A | 4.20e-03 | 0.9819 |
| rs8074437 | 38076137 | -0.1687 | T | G | 5.44e-03 | 0.9819 |
| rs4065275 | 38080865 | -0.1673 | A | G | 4.64e-03 | 0.9819 |
| rs12603332 | 38082807 | -0.1636 | T | C | 2.36e-03 | 0.9819 |

SUPPLEMENTARY DATA

**Supplementary Table 8.** Most likely variants causally associated with T1D at the *IL2RA* locus from GUESSFM fine mapping analysis.

| Variant | Position (gr37) | Log-odds ratio | Reference allele | Effect allele | Variant posterior probability | Group posterior probability | GUESSFM group from Wallace et. al.* |
|---|---|---|---|---|---|---|---|
| rs12722563 | 6069561 | -0.4317 | G | A | 1.44e-04 | 0.9995 | A |
| rs12722558 | 6070276 | -0.415 | A | T | 6.53e-05 | 0.9995 | A |
| rs12722552 | 6071347 | -0.4346 | C | T | 1.22e-04 | 0.9995 | A |
| rs12722522 | 6078553 | -0.4843 | G | A | 2.39e-02 | 0.9995 | A |
| rs12722508 | 6088743 | -0.4874 | A | T | 3.36e-02 | 0.9995 | A |
| rs7909519 | 6089841 | -0.4943 | T | G | 1.02e-01 | 0.9995 | A |
| rs61839660 | 6094697 | -0.5367 | C | T | 6.02e-02 | 0.9995 | A |
| rs12722496 | 6096667 | -0.5012 | A | G | 6.72e-01 | 0.9995 | A |
| rs12722495 | 6097283 | -0.4903 | T | C | 1.03e-01 | 0.9995 | A |
| rs79092647 | 6109345 | -0.4925 | CAAA | C | 1.14e-03 | 0.9995 | A |
| rs41295049 | 6109676 | -0.4869 | G | A | 1.76e-03 | 0.9995 | A |
| rs41295061 | 6114660 | -0.4772 | C | A | 4.95e-04 | 0.9995 | A |
| rs41295065 | 6116975 | -0.4785 | G | A | 5.97e-04 | 0.9995 | A |
| rs35285258 | 6118770 | -0.1373 | C | T | 3.55e-01 | 0.9973 | C |
| rs11594656 | 6122009 | -0.1398 | T | A | 6.43e-01 | 0.9973 | C |
| rs6602437 | 6130077 | 0.1346 | T | C | 8.97e-01 | 0.9973 | E |
| rs34975410 | 6130122 | 0.1209 | TA | T | 1.01e-01 | 0.9973 | E |

*Groups defined in [12] named 'A'-'F', of which 'A', 'C', 'E' and 'F' were found to be type 1 diabetes associated. The group 'F' variants were removed from the stochastic search in this analysis due to difference in imputation quality between cases and controls of >1%.

SUPPLEMENTARY DATA

**Supplementary Table 9.** Most likely variants causally associated with T1D at the *THEMIS* locus from GUESSFM fine mapping analysis.

| Variant | Position (gr37) | Log-odds ratio | Reference allele | Effect allele | Variant posterior probability | Group posterior probability |
|---|---|---|---|---|---|---|
| rs67707912 | 128217774 | -0.204 | T | C | 1.47e-02 | 0.9698 |
| rs13204742 | 128245765 | -0.2001 | G | T | 1.10e-02 | 0.9698 |
| rs6939352 | 128266250 | -0.1984 | T | G | 3.96e-02 | 0.9698 |
| rs9491889 | 128270067 | -0.1998 | C | T | 4.48e-02 | 0.9698 |
| rs9491890 | 128270123 | -0.2001 | G | A | 4.65e-02 | 0.9698 |
| rs9491891 | 128277151 | -0.2025 | A | G | 5.99e-02 | 0.9698 |
| rs147626184 | 128277275 | -0.2024 | C | CAACTTGAAT | 5.45e-02 | 0.9698 |
| rs118097399 | 128278233 | -0.204 | C | T | 6.85e-02 | 0.9698 |
| rs9491892 | 128280358 | -0.196 | T | G | 3.44e-02 | 0.9698 |
| rs9482848 | 128280375 | -0.195 | A | T | 2.94e-02 | 0.9698 |
| rs9491893 | 128280931 | -0.2047 | G | A | 7.42e-02 | 0.9698 |
| rs113297984 | 128286301 | -0.1943 | G | A | 2.50e-02 | 0.9698 |
| rs72973797 | 128286386 | -0.1998 | G | A | 4.69e-02 | 0.9698 |
| rs72973800 | 128287158 | -0.1989 | C | T | 3.91e-02 | 0.9698 |
| rs761332 | 128287848 | -0.198 | G | A | 3.85e-02 | 0.9698 |
| rs9482849 | 128288536 | -0.1973 | T | C | 3.65e-02 | 0.9698 |
| rs12111314 | 128289214 | -0.2016 | C | T | 4.89e-02 | 0.9698 |
| rs11753289 | 128291681 | -0.1965 | T | G | 3.24e-02 | 0.9698 |
| rs9482850 | 128293506 | -0.2011 | C | T | 4.98e-02 | 0.9698 |
| rs9482851 | 128293634 | -0.1995 | C | T | 3.86e-02 | 0.9698 |
| rs72975913 | 128293932 | -0.2004 | C | A | 4.60e-02 | 0.9698 |
| rs72975916 | 128294055 | -0.2 | C | T | 4.48e-02 | 0.9698 |
| rs7738609 | 128295502 | -0.1888 | C | T | 1.35e-02 | 0.9698 |
| rs138300818 | 128297022 | -0.1825 | T | TG | 8.45e-03 | 0.9698 |
| rs3901020 | 128297604 | -0.187 | C | G | 1.23e-02 | 0.9698 |
| rs4510698 | 128297611 | -0.1865 | C | T | 1.16e-02 | 0.9698 |

SUPPLEMENTARY DATA

**Supplementary Table 10.** Most likely variants causally associated with T1D at the *IL10* locus from GUESSFM fine mapping analysis.

| Variant | Position (gr37) | Log-odds ratio | Reference allele | Effect allele | Variant posterior probability | Group posterior probability |
|---|---|---|---|---|---|---|
| rs3024505 | 206939904 | -0.2486 | G | A | 3.70e-01 | 0.9954 |
| rs3024495 | 206942413 | -0.2476 | C | T | 2.52e-01 | 0.9954 |
| rs3024493 | 206943968 | -0.2485 | C | A | 3.68e-01 | 0.9954 |
| rs3122605 | 206955041 | -0.2172 | A | G | 5.45e-03 | 0.9954 |

SUPPLEMENTARY DATA

**Supplementary Table 11.** Chip heritability estimates by age-at-diagnosis group under various disease prevalence assumptions.

| **Disease prevalence (%) (<7,7-13,≥13)** | **<7 including MHC (95% CI)** | **7-13 including MHC (95% CI)** | **≥13 including MHC (95% CI)** | **<7 excluding MHC (95% CI)** | **7-13 excluding MHC (95% CI)** | **≥13 excluding MHC (95% CI)** |
|---|---|---|---|---|---|---|
| 0.4,0.4,0.4 | 0.366 (0.346, 0.386) | 0.301 (0.284, 0.319) | 0.233 (0.206, 0.260) | 0.209 (0.188, 0.229) | 0.178 (0.160, 0.195) | 0.090 (0.069, 0.110) |
| 0.5,0.3,0.3 | 0.383 (0.362, 0.40) | 0.285 (0.268, 0.301) | 0.220 (0.195, 0.245) | 0.218 (0.197, 0.239) | 0.168 (0.152, 0.184) | 0.085 (0.065, 0.104) |
| 0.5,0.2,0.2 | 0.383 (0.362, 0.40) | 0.264 (0.249, 0.280) | 0.204 (0.180, 0.228) | 0.180 (0.197, 0.239) | 0.156 (0.141, 0.171) | 0.079 (0.061, 0.097) |

SUPPLEMENTARY DATA

**Supplementary References**


1. Onengut-Gumuscu, S. *et al.* Fine mapping of type 1 diabetes susceptibility loci and evidence for colocalization of causal variants with lymphoid gene enhancers. *Nat. Genet.* **47**, 381–6 (2015).
2. Bain, S. C., Todd, J. A. & Barnett, A. H. The British Diabetic Association - Warren Repository. *Autoimmunity* **7**, 83–85 (1990).
3. Inshaw, J. R. J., Walker, N. M., Wallace, C., Bottolo, L. & Todd, J. A. The chromosome 6q22.33 region is associated with age at diagnosis of type 1 diabetes and disease risk in those diagnosed under 5 years of age. *Diabetologia* **61**, 147–157 (2018).
4. Qiao, Q. *et al.* A genome-wide scan for type 1 diabetes susceptibility genes in nuclear families with multiple affected siblings in Finland. *BMC Genet.* **8**, (2007).
5. Manichaikul, A. *et al.* Robust relationship inference in genome-wide association studies. *Bioinformatics* **26**, 2867–2873 (2010).
6. Mahajan, A. *et al.* Fine-mapping type 2 diabetes loci to single-variant resolution using high-density imputation and islet-specific epigenome maps. *Nat. Genet.* **50**, 1505–1513 (2018).
7. Chang, C. C. *et al.* Second-generation PLINK : rising to the challenge of larger and richer datasets. *Gigascience* **4**, (2015).
8. Banjamini, Y. & Hochberg, Y. Controlling the False Discovery Rate : a Practical and Powerful Approach to Multiple Testing. *J. R. Stat. Soc. B* **57**, 289–300 (1995).
9. Giambartolomei, C. *et al.* Bayesian Test for Colocalisation between Pairs of Genetic Association Studies Using Summary Statistics. *PLoS Genet.* **10**, (2014).
10. Fortune, M. D. *et al.* Statistical colocalization of genetic risk variants for related autoimmune diseases in the context of common controls. *Nat. Genet.* **47**, 839–846 (2015).
11. Burren, O. S. *et al.* Chromosome contacts in activated T cells identify autoimmune disease candidate genes. *Genome Biol.* **18**, 165 (2017).
12. Wallace, C. *et al.* Dissection of a Complex Disease Susceptibility Region Using a Bayesian Stochastic Search Approach to Fine Mapping. *PLOS Genet.* **11**, e1005272 (2015).
13. Inshaw, J. R. J., Cutler, A. J., Burren, O. S., Stefana, M. I. & Todd, J. A. Approaches and advances in the genetic causes of autoimmune disease and their implications. *Nat. Immunol.* **19**, 674–684 (2018).
14. Miguel-Escalada, I. *et al.* Human pancreatic islet 3D chromatin architecture provides insights into the genetics of type 2 diabetes. *bioRxiv* (2018).
15. Fernandez, J. M. *et al.* The BLUEPRINT Data Analysis Portal. *Cell Syst.* **3**, 491–495 (2016).
16. Turk, B., Turk, D. & Turk, V. Lysosomal cysteine proteases: more than scavengers. *Biochim. Biophys. Acta* **1477**, 98–111 (2000).
17. Wang, Y. *et al.* How C-terminal additions to insulin B-chain fragments create superagonists for T cells in mouse and human type 1 diabetes. *Sci. Immunol.* **4**, eaav7517 (2019).
18. Ueno, T. *et al.* Processing of Pulmonary Surfactant Protein B by Napsin and Cathepsin H*. *J. Biol. Chem.* **279**, 16178–16184 (2004).
19. Angelo, M. E. D. *et al.* Cathepsin H Is an Additional Convertase of Pro-granzyme B. *J. Biol. Chem.* **285**, 20514–20519 (2010).
20. Qi, R., Singh, D. & Kao, C. C. Proteolytic Processing Regulates Toll-like Receptor 3 Stability and Endosomal Localization. *J. Biol. Chem.* **287**, 32617–32629 (2012).
21. Garcia-cattaneo, A., Gobert, F., Müller, M., Toscano, F. & Flores, M. Cleavage of Toll-like receptor 3 by cathepsins B and H is essential for signaling. *PNAS* **109**, 9053–9058 (2012).
22. Okada, R., Zhang, X., Harada, Y., Wu, Z. & Nakanishi, H. Cathepsin H deficiency in mice induces excess Th1 cell activation and early-onset of EAE though impairment of toll-like receptor 3 cascade. *Inflamm. Res.* **67**, 371–374 (2018).

23. Guo, H. *et al.* Integration of disease association and eQTL data using a Bayesian colocalisation approach highlights six candidate causal genes in immune-mediated diseases. *Hum. Mol. Genet.* **24**, 3305–3313 (2015).
24. Kim, Y., Nakanishi, G., Lewandoski, M. & Jetten, A. M. GLIS3 , a novel member of the GLIS subfamily of Kruppel-like zinc finger proteins with repressor and activation functions. *Nucleic Acids Res.* **31**, 5513–5525 (2003).
25. Yang, Y., Chang, B. H. & Chan, L. Sustained expression of the transcription factor GLIS3 is required for normal beta cell function in adults. *EMBO Mol. Med.* **5**, 92–104 (2013).
26. Nogueira, T. C. *et al.* GLIS3, a Susceptibility Gene for Type 1 and Type 2 Diabetes , Modulates Pancreatic Beta Cell Apoptosis via Regulation of a Splice Variant of the BH3-Only Protein Bim. *PLoS Genet.* **9**, e1003532 (2013).
27. Dooley, J. *et al.* Genetic predisposition for beta cell fragility underlies type 1 and type 2 diabetes. *Nat. Genet.* **48**, 519–527 (2016).
28. John, L. B. & Ward, A. C. The Ikaros gene family : Transcriptional regulators of hematopoiesis and immunity. *J. Mol. Immunol.* **48**, 1272–1278 (2011).
29. Wang, J. *et al.* Aiolos Regulates B Cell Activation and Maturation to Effector State. *Immunity* **9**, 543–553 (1998).
30. Cortés, M. & Georgopoulos, K. Aiolos Is Required for the Generation of High Affinity Bone Marrow Plasma Cells Responsible for Long-Term Immunity. *J. Exp. Med.* **199**, 209–219 (2004).
31. Quintana, F. J. *et al.* Aiolos promotes TH17 differentiation by directly silencing Il2 expression. *Nat. Immunol.* **13**, 770–777 (2012).
32. Kwon, H., Chen, H., Mathis, D. & Benoist, C. Different molecular complexes that mediate transcriptional induction and repression by FoxP3. *Nat. Immunol.* **18**, 1238–1248 (2017).
33. Davis, D., Kannan, M. & Wattenberg, B. Orm / ORMDL proteins: Gate guardians and master regulators. *Adv. Biol. Regul.* **70**, 3–18 (2018).
34. Carreras-Sureda, A. *et al.* ORMDL3 modulates store-operated calcium entry and lymphocyte activation. *Hum. Mol. Genet.* **22**, 519–530 (2013).
35. Schmiedel, B. J. *et al.* 17q21 asthma-risk variants switch CTCF binding and regulate IL-2 production by T cells. *Nat. Commun.* **7**, (2016).
36. Feng, S., Fox, D. & Man, S. M. Mechanisms of Gasdermin Family Members in Inflammasome Signaling and Cell Death. *J. Mol. Biol.* **430**, 3068–3080 (2018).
37. Panganiban, R. A. *et al.* A functional splice variant associated with decreased asthma risk abolishes the ability of gasdermin B to induce epithelial cell pyroptosis. *J. Allergy Clin. Immunol.* **142**, 1469–1478 (2018).
38. Mingari, M. *et al.* Human interleukin-2 promotes proliferation of activated B cells via surface receptors similar to those of activated T cells. *Nature* **312**, 641–643 (1984).
39. Spolski, R., Li, P. & Leonard, W. J. Biology and regulation of IL-2: from molecular mechanisms to human therapy. *Nat. Rev. Immunol.* **18**, 648–659 (2018).
40. Stanford, S. M., Rapini, N. & Bottini, N. Regulation of TCR signalling by tyrosine phosphatases: from immune homeostasis to autoimmunity. *Immunology* **137**, 1–19 (2012).
41. Mehta, M. *et al.* Themis-associated phosphatase activity controls signaling in T cell development. *PNAS* **115**, E11331–E11340 (2018).
42. Choi, S., Cornall, R., Lesourne, R. & Love, P. E. THEMIS : Two Models, Different Thresholds. *Trends Immunol.* **38**, 622–632 (2017).
43. Brockmeyer, C. *et al.* T cell receptor (TCR)-induced tyrosine phosphorylation dynamics identifies THEMIS as a new TCR signalosome component. *J. Biol. Chem.* **286**, 7535–7547 (2011).
44. Paster, W. *et al.* A THEMIS: SHP 1 complex promotes T-cell survival. *EMBO J.* **34**, 393–409 (2015).
45. Moore, K. W., Malefyt, R. D. W., Robert, L. & Garra, A. O. INTERLEUKIN-10 AND THE

INTERLEUKIN -10 RECEPTOR. *Annu. Rev. Immunol.* **19**, 683–765 (2001).
46. Roncarolo, M. G., Gregori, S., Bacchetta, R., Battaglia, M. & Gagliani, N. The Biology of T Regulatory Type 1 Cells and Their Therapeutic Application in Immune-Mediated Diseases. *Immunity* **49**, 1004–1019 (2018).
47. Mauri, C. & Menon, M. Human regulatory B cells in health and disease: therapeutic potential. *J. Clin. Invest.* **127**, 772–779 (2017).
48. Ren, B. *et al.* Interleukin 10 (IL-10) and Viral IL-10 Strongly Reduce Antigen-specific Human T Cell Proliferation by Diminishing the Antigen-presenting Capacity of Monocytes via Downregulation of Class II Major Histocompatibility Complex Expression. *J. Exp. Med.* **174**, 915–924 (1991).
49. Groux, H., Bigler, M., de Vries, J. E. & Roncarolo, M. Interleukin-10 Induces a Long-Term Antigen-specific Anergic State in Human CD4+ T Cells. *J. Exp. Med.* **184**, 19–29 (1996).
50. Rousset, F. *et al.* Interleukin 10 is a potent growth and differentiation factor for activated human B lymphocytes. *PNAS* **89**, 1890–1893 (1992).
51. Wang, H., Coligan, J. E. & Morse, H. C. Emerging Functions of Natural IgM and Its Fc Receptor FCMR in Immune Homeostasis. *Front. Immunol.* **7**, 99 (2016).
52. Ouchida, R. *et al.* Critical role of the IgM Fc receptor in IgM homeostasis , B-cell survival , and humoral immune responses. *PNAS* **109**, E2699–E2706 (2012).
53. Yu, J. *et al.* Surface receptor Toso controls B cell – mediated regulation of T cell immunity. *J. Clin. Invest.* **128**, 1820–1836 (2018).
54. Nguyen, T. T. T., Graf, B. A., Randall, T. D. & Baumgarth, N. sIgM - FcμR interactions regulate early B cell activation and plasma cell development after influenza virus infection. *J. Immunol.* **199**, 1635–1646 (2017).
55. Javierre, B. M. *et al.* Lineage-Specific Genome Architecture Links Enhancers and Non-coding Disease Variants to Target Gene Promoters. *Cell* **167**, 1369–1384 (2016).
56. Eizirik, L. *et al.* The Human Pancreatic Islet Transcriptome: Expression of Candidate Genes for Type 1 Diabetes and the Impact of Pro-Inflammatory Cytokines. *PLoS Genet.* **8**, e1002552 (2012).
57. Võsa, U. *et al.* Unraveling the polygenic architecture of complex traits using blood eQTL meta-analysis. *bioRxiv* 1–57 (2018).